AD_____

Award Number: W81XWH-09-1-0184

TITLE: Defining the Role of BTLA in Breast Cancer Immunosurveillance and Selective Targeting of the BTLA-HVEM-LIGHT Costimulatory System

PRINCIPAL INVESTIGATOR: William Gillanders

CONTRACTING ORGANIZATION: Washington University
Saint Louis, MO 63130-4862

REPORT DATE: May 2012

TYPE OF REPORT: Final

PREPARED FOR: U.S. Army Medical Research and Materiel Command
Fort Detrick, Maryland 21702-5012

REPORT DOCUMENTATION PAGE

Form Approved
OMB No. 0704-0188

1. REPORT DATE	**2. REPORT TYPE**	**3. DATES COVERED**
May 2012	Final	1 May 2009 – 30 April 2012

4. TITLE AND SUBTITLE
Defining the Role of B TLA in Breast Cancer Immunosurveillance and Selective Targeting of the B TLA- HVEM- Light Costimulatory System

5a. CONTRACT NUMBER

5b. GRANT NUMBER
W81XWH-09-1-0184

5c. PROGRAM ELEMENT NUMBER

6. AUTHOR(S)
William Gillanders

E-Mail: gillandersw@wudosis.wustl.edu

5d. PROJECT NUMBER

5e. TASK NUMBER

5f. WORK UNIT NUMBER

7. PERFORMING ORGANIZATION NAME(S) AND ADDRESS(ES)
Washington University
Saint Louis MO 63130-4862

8. PERFORMING ORGANIZATION REPORT NUMBER

9. SPONSORING / MONITORING AGENCY NAME(S) AND ADDRESS(ES)
U.S. Army Medical Research and Materiel Command
Fort Detrick, Maryland 21702-5012

10. SPONSOR/MONITOR'S ACRONYM(S)

11. SPONSOR/MONITOR'S REPORT NUMBER(S)

12. DISTRIBUTION / AVAILABILITY STATEMENT
Approved for Public Release; Distribution Unlimited

13. SUPPLEMENTARY NOTES

14. ABSTRACT- Costimulatory (CD28, ICOS) and inhibitory (CTLA4, PD-1) molecules of the CD28 receptor family provide critical secondary signals regulating the balance between protective immunity and tissue injury. We recently cloned B- and T-lymphocyte attenuator (BTLA), the third inhibitory receptor of the CD28 family expressed on lymphocytes. Using BTLA-deficient mice and monoclonal antibodies specific for BTLA that we generated, we have studied several in vivo models of infection and autoimmunity, showing the importance of BTLA in regulating immune responses. The hypothesis of this application was that BTLA contributes to the inhibition of breast cancer immunosurveillance, and selective targeting of the BTLA-LIGHT-HVEM costimulatory system can enhance breast cancer immunity. The overall aim was to evaluate the role of BTLA in breast cancer immunosurveillance, and develop novel therapeutics targeting the BTLA-LIGHT-HVEM costimulatory system. We observed that (1) various HVEM mutants were generated that ablate binding of BTLA but preserve binding of LIGHT. However, wild type HVEM but not mutant HVEM is an effective molecular adjuvant in the context of DNA vaccination, (2) expression of BTLA in human breast cancers of various histologic types is restricted to only 1-3% of CD8 T cells in tumor and tumor-draining lymph nodes, (3) in a murine graft-versus-host disease (GVHD) model anti-BTLA therapy permanently prevented GVHD through blockade of alloreactive donor T cells, and, (4) BTLA is highly expressed on a subset of dendritic cells uniquely qualified for cross-presentation of antigen and generation of effective T cell immunity. In summary, progress has been made towards the goal of defining the role of BTLA in breast cancer immunosurveillance. BTLA is minimally expressed on CD8 T cells infiltrating human breast cancer; however, the surprising finding that a subset of dendritic cells expresses high levels of BTLA suggest a role for BTLA-LIGHT-HVEM interactions in CD8 T cell activation. Mechanistic studies in a model of GVHD confirm the importance of the BTLA-LIGHT-HVEM costimulatory system, and will help direct future studies.

15. SUBJECT TERMS- none provided

16. SECURITY CLASSIFICATION OF:			**17. LIMITATION OF ABSTRACT**	**18. NUMBER OF PAGES**	**19a. NAME OF RESPONSIBLE PERSON**
					USAMRMC
a. REPORT	**b. ABSTRACT**	**c. THIS PAGE**			**19b. TELEPHONE NUMBER** *(include area code)*
U	U	U	UU		

TABLE OF CONTENTS

INTRODUCTION

BACKGROUND: In the last decade, considerable progress has been made in understanding the complex regulatory networks that control immune responses. Regulating the extent, quality and duration of immune responses is critical for balancing protective immunity and tissue injury. Costimulatory (CD28, ICOS) and inhibitory (CTLA4, PD-1) molecules of the CD28 receptor family provide critical secondary signals regulating this balance, and recent work has uncovered critical roles for CTLA4 and PD-1 in restraining immune responses in chronic viral infection and malignancy. We recently cloned B- and T-lymphocyte attenuator (BTLA), the third inhibitory receptor of the CD28 family expressed on lymphocytes. Using BTLA-deficient mice and monoclonal antibodies specific for BTLA that we generated, we have studied several in vivo models of infection and autoimmunity, showing the importance of BTLA in regulating immune responses. Several lines of evidence suggest that inhibitory molecules such as CTLA-4 and PD-1 limit cancer immunosurveillance.

OBJECTIVE/HYPOTHESIS: The hypothesis of this application is that BTLA contributes to the inhibition of breast cancer immunosurveillance, and selective targeting of the BTLA-LIGHT-HVEM costimulatory system can enhance breast cancer immunity.

SPECIFIC AIMS:

(1) Define the role of BTLA in breast cancer immunosurveillance.

(2) Determine if inhibitory molecules of the CD28 receptor family function as redundant immunologic checkpoints in breast cancer immunosurveillance.

(3) Develop novel therapeutics to successfully dissociate T cell costimulation and inhibition in the BTLA-LIGHT-HVEM costimulatory system.

PROGRESS: The award was in the format of a Synergistic Idea Award to William E. Gillanders, M.D., a breast cancer surgeon, and Kenneth Murphy, M.D., Ph.D., a basic immunologist. The current report represents a final report for the entire period including the no-cost extension period in which Dr. Gillanders continued the studies.

The overall aim was to evaluate the role of BTLA in breast cancer immunosurveillance, and develop novel therapeutics targeting the BTLA-LIGHT-HVEM costimulatory system. During the course of the study period, we have made a number of important observations that provide important insights into the role of BTLA in breast cancer immunosurveillance, into the basic biology of BTLA, and into mechanisms of antigen presentation following DNA vaccination: (1) We performed studies in human breast cancer specimens demonstrating that expression of BTLA in human breast cancers of various histologic types is restricted to only 1-3% of CD8 T cells in primary tumors and tumor-draining lymph nodes (Please see Appendix 1). These studies suggest that BTLA may only have a limited role in breast cancer immunosurveillance, the key question addressed in Specific Aim 1. (2) Various HVEM mutants were generated that ablate binding of BTLA but preserve binding of LIGHT. These constructs were constructed in an attempt to dissociate T cell costimulation and inhibition in the BTLA-LIGHT-HVEM costimulatory system. However, we observed that wildtype HVEM, but not mutant HVEM,

is an effective molecular adjuvant in the context of DNA vaccination. This surprising finding was not predicted by our original hypothesis (Please see Appendix 3, 4). Of note, this surprising finding provided key insights that lead directly to important studies of BTLA biology in graft versus host disease, and the mechanisms of antigen presentation following DNA vaccination. Specifically, we found that (3) In a murine graft-versus-host disease (GVHD) model anti-BTLA therapy permanently prevented GVHD through blockade of alloreactive donor T cells, and (4) BTLA is highly expressed on a subset of dendritic cells uniquely qualified for cross-presentation of antigen and generation of effective T cell immunity. We are particularly excited by the latter finding and were recently successful in securing funds to continue these studies.

BODY

Specific Aim 1: To assess the role of BTLA in breast cancer immune surveillance we determined expression of BTLA in peripheral blood, lymph nodes, and tumor tissue in human breast cancer patients. Both flow cytometry and immunohistochemistry was performed. Co-staining for CD8 showed very few (<5%) of CD8 T cells express BTLA. However, BTLA is highly expressed on a subset of dendritic cells involved in cross presentation. Please see Appendix #1 for details.

Specific Aims 2A, 2B: Progress in the studies outlined in these Aims were hampered by the fact that our BALB/c-*neu*T breeding colony had to be re-established, causing a significant delay in establishing a BALB/c-*neu*T/BTLA$^{-/-}$ strain. Once we successfully expanded our colony of BALB/c-*neu*T mice, breeding of BALB/c-*neu*T mice to BTLA-deficient mice was initiated. No spontaneous tumors from BALB/c-*neu*T mice have been evaluated as all animals of sufficient age and appropriate genetic background were used to cross with BTLA-deficient mice or for vaccination experiments outlined in 3C. Breeding BAL/c-neuT to BTLA-deficient mice proved very difficult. While we did generate F1 mice, backcrossing F1 to BTLA$^{-/-}$ mice appeared lethal. These studies will be continued using funds from other sources.

Specific Aims 3A, 3B: LIGHT signaling through HVEM results in CD28-independent T cell costimulation, dramatically enhancing antitumor and other cell-mediated immune responses, whereas BTLA signaling through HVEM induces inhibitory signals. We earlier reported the successful creation of three different HVEM mutants using site-directed mutagenesis: P17A, Y23A, and V36A with the goal to ablate binding of BTLA but preserve binding of LIGHT. The mutant constructs were initially expressed in CHO cells to assess binding of HVEM and BTLA. Subsequently, the mutant constructs were cloned into pcDNA3 vector for further functional validation. *In vitro* studies confirm that P17A successfully ablates BTLA interaction. Functional analysis In three independent experiments showed the surprising finding that administration of wildtype HVEM enhances the immune response to OVA cDNA, but the P17A mutant HVEM unexpectedly did not. Please see Appendices 3 and 4 for additional details.

Specific Aim 3C: Wildtype (wt) and mutant HVEM constructs were successfully cloned into the pcDNA3 plasmid DNA vector, and expression was confirmed. To assess their ability to enhance DNA vaccination, several vaccination protocols were developed based on the model antigen, ovalbumin (OVA). Surprisingly, our data suggest that wildtype, but not mutant HVEM, is an effective molecular adjuvant in the context of DNA vaccination. In addition, we have validated a clinically relevant breast cancer vaccine model in our laboratory to test the HVEM constructs. This model system is based on the BALB/c-*neu*T genetically engineered murine model of breast cancer. BALB/c-*neu*T mice express the transforming rat oncogene HER2/neu under the mouse mammary tumor virus (MMTV) promoter. These mice spontaneously develop breast cancer with a well-defined progression from dysplasia, to *in situ* carcinoma, to overt invasive carcinoma similar to human disease. We have established a cancer vaccine model, where DNA vaccination with conventional (HER2/neu cDNA vaccine), or experimental (HER2/neu single chain trimer DNA vaccines, K^d/L^d SCT) cancer vaccines can protect against tumor challenge (TUBO). This represents an ideal platform for testing the wildtype and mutant

HVEM constructs. In two independent experiments vaccination with wild type HVEM DNA and K^d/L^d SCT DNA showed a down regulation of the immune response in the presence of HVEM wild type DNA, contrary to our observations using OVA cDNA. These findings suggest the role of HVEM-BTLA signaling is complex and requires more studies to elucidate. Please see Appendix #5 for additional details.

Additional Studies I: Given the surprising results noted above (Specific Aim 3C), additional mechanistic studies of BTLA biology have been performed in the Murphy laboratory, pending availability of BALB/c-*neu*T mice of the appropriate age and genetic background. These studies of the BTLA-LIGHT-HVEM costimulatory system have been carried out in a murine model of graft-versus-host disease. Based upon the likely similarity of the mechanisms of action of BTLA in breast cancer-specific T cells and in expanding T cells in the GVHD model, we have carried out a series of studies into the mechanism and effects of BTLA-directed immunotherapy. In GVHD, T cells expanding following bone marrow transplantation not only manifest graft-versus-host disease, but also mediate important antitumor effects. Therefore, we have carried out an analysis to evaluate the role of BTLA-directed therapy in this setting. The model used is the fully irradiated GVHD model. Two forms of this were tested, including a fully MHC-mismatched model of B6 transfer into BALB/c recipients, or a parental into F1 model. In both cases, either lethal or chronic GVHD is established, concurrent with significant weight loss, and a permanent mucosal inflammatory disease in the gut and elsewhere. Our essential finding is that the treatment of recipient mice with a single injection of anti-BTLA antibody (6A6) results in permanent prevention of GVHD. Since last year's report, we have further identified that the mechanism of anti-BTLA treatment at the time of bone marrow transplantation is a selective blockade of alloreactive donor T cells, without a blockade in the expansion and effector activities of normally protective and pathogen-specific donor T cells. This work has now been published in the *Journal of Experimental Medicine*. Of relevance to the current proposal, we have found that HVEM is not involved in the mechanisms of the beneficial effects of BTLA-directed therapy. During homeostatic expansion, HVEM is not engaged to limit the expansion of effector T cells after BMT. This observation may alter our future focus to concentrate on BTLA rather than HVEM manipulations in considering ways to augment anti-tumor vaccinations. Please see Appendix #6 for manuscript published in Journal of Experimental Medicine.

Additional Studies II: While our studies on BTLA expression in CD8 T cells infiltrating human breast tumors yielded disappointing results, we were surprised to detect substantial BTLA expression in dendritic cells. Further study through flow cytometry showed that expression of BTLA is most prominent in a subset of dendritic cells expressing CD8α/CD103 in mice and Clec9A in humans. Recent studies by the Murphy and Gillanders laboratories have characterized this subset of dendritic cells as the cells uniquely capable of cross-presentation and cross-dressing, and priming of CD8 T cells after vaccination. Mice deficient in this subset of dendritic cells failed to stimulate naïve CD8 T cells following DNA or cellular vaccination. Please see Appendix #7 for manuscript published in PNAS and Appendix #8 for additional data.

Problem Areas: We encountered an unforeseen problem when the postdoctoral fellow recruited to work on this project left unexpectedly due to family health issues. This individual ultimately resigned the position, and

this unexpected departure ultimately resulted in having to re-establish the BALB/c-neuT and related mouse colonies. We successfully recruited another postdoctoral fellow to fill the position. This individual has a strong background in tumor immunology and vaccine development. In addition, towards the end of year two we recruited a second postdoctoral fellow to work on this project. This individual has obtained a postdoctoral fellowship award from the Swiss National Foundation, and the main focus of her proposed studies was the studies described in Specific Aims 1 and 2. An additional problem was the generation of BALB/c-neuT/BTLA$^{-/-}$ mice. Crossing F1 to BTLA$^{-/-}$ mice proved lethal.

KEY RESEARCH ACCOMPLISHMENTS

(1) Assessment of BTLA expression on T lymphocytes in human breast cancer by flow cytometry and immunohistochemistry. The prevalence of $CD8^+BTLA^+$ T cells in human breast cancer is less than 5%.

(2) Successful creation of wildtype and mutant HVEM constructs, and successful cloning of these constructs into retroviral and plasmid DNA vectors.

(3) Assessment of the adjuvant effect of wildtype and mutant HVEM constructs as novel molecular adjuvants in a DNA vaccine model. Wildtype HVEM does appear to be an effective molecular adjuvant.

(4) Successful establishment and validation of a clinically relevant breast cancer DNA vaccine model, representing an ideal platform for testing the wildtype and mutant HVEM constructs.

(5) Identification of an effect of BTLA-directed therapy in the treatment of graft-versus-host disease, which may have important clinical relevance in breast cancer and other diseases.

(6) Demonstration that CD8α dendritic cells, and cross-presentation, are essential for priming CD8 T cell responses following DNA vaccination.

(7) Identification of high levels of BTLA on a subset of both mouse and human dendritic cells involved in cross-presentation of antigen to CD8 T cells.

REPORTABLE OUTCOMES

The manuscript: “Targeting of B and T lymphocyte associated (BTLA) prevents graft-versus-host disease without global immunosuppression” was published in the *Journal of Experimental Medicine* (JEM 2010, 207:2552). Please see Appendix # 6.

The manuscript: “Cross-dressed CD8α+ dendritic cells prime CD8+ T cells following vaccination” was published in the *Proceedings of the National Academy of Sciences* (PNAS 109(31):12716-21). Please see Appendix # 7.

CONCLUSIONS

Progress has been made towards the goal of defining the role of BTLA in breast cancer immunosurveillance. BTLA is minimally expressed on CD8 T cells infiltrating human breast cancer; however, the surprising finding that a subset of dendritic cells expresses high levels of BTLA suggest a role for BTLA-LIGHT-HVEM interactions in CD8 T cell activation. Mechanistic studies in a model of GVHD confirm the importance of the BTLA-LIGHT-HVEM costimulatory system, and will help direct future studies.

REFERENCES

1. Hildner, K., B.T. Edelson, W.E. Purtha, M. Diamond, H. Matsushita, M. Kohyama, B. Calderon, B.U. Schraml, E.R. Unanue, M.S. Diamond, R.D. Schreiber, T.L. Murphy, and K.M. Murphy. 2008. Batf3 deficiency reveals a critical role for CD8alpha+ dendritic cells in cytotoxic T cell immunity. *Science* 322:1097-1100.
2 Torti, N., S.M. Walton, K.M. Murphy, and A. Oxenius. Batf3 transcription factor-dependent DC subsets in murine CMV infection: differential impact on T-cell priming and memory inflation. *Eur J Immunol* 41:2612-2618.
3. Dunn, G.P., A.T. Bruce, K.C. Sheehan, V. Shankaran, R. Uppaluri, J.D. Bui, M.S. Diamond, C.M. Koebel, C. Arthur, J.M. White, and R.D. Schreiber. 2005. A critical function for type I interferons in cancer immunoediting. *Nat Immunol* 6:722-729.
4. Shankaran, V., H. Ikeda, A.T. Bruce, J.M. White, P.E. Swanson, L.J. Old, and R.D. Schreiber. 2001. IFNgamma and lymphocytes prevent primary tumour development and shape tumour immunogenicity. *Nature* 410:1107-1111.
5. Li, L., S. Kim, J.M. Herndon, P. Goedegebuure, T.P. Fleming, T.H. Hansen, K.M. Murphy, and W.E. Gillanders. 2012. Cross-dressed CD8α+ dendritic cells prime CD8+ T cells following vaccination. *Proceedings of the National Academy of Sciences*, 109(31):12716-21.
6. Watanabe, N., M. Gavrieli, J.R. Sedy, J. Yang, F. Fallarino, S.K. Loftin, M.A. Hurchla, N. Zimmerman, J. Sim, X. Zang, T.L. Murphy, J.H. Russell, J.P. Allison, and K.M. Murphy. 2003. BTLA is a lymphocyte inhibitory receptor with similarities to CTLA-4 and PD-1. *Nat Immunol* 4:670-679.
7. Albring, J.C., M.M. Sandau, A.S. Rapaport, B.T. Edelson, A. Satpathy, M. Mashayekhi, S.K. Lathrop, C.S. Hsieh, M. Stelljes, M. Colonna, T.L. Murphy, and K.M. Murphy. 2010. Targeting of B and T lymphocyte associated (BTLA) prevents graft-versus-host disease without global immunosuppression. *The Journal of experimental medicine* 207:2551-2559.
8. Gavrieli, M., J. Sedy, C.A. Nelson, and K.M. Murphy. 2006. BTLA and HVEM cross talk regulates inhibition and costimulation. *Advances in immunology* 92:157-185.
9. Hurchla, M.A., J.R. Sedy, M. Gavrieli, C.G. Drake, T.L. Murphy, and K.M. Murphy. 2005. B and T lymphocyte attenuator exhibits structural and expression polymorphisms and is highly Induced in anergic CD4+ T cells. *Journal of immunology* 174:3377-3385.
10. Hurchla, M.A., J.R. Sedy, and K.M. Murphy. 2007. Unexpected role of B and T lymphocyte attenuator in sustaining cell survival during chronic allostimulation. *Journal of immunology* 178:6073-6082.
11. Murphy, K.M., C.A. Nelson, and J.R. Sedy. 2006. Balancing co-stimulation and inhibition with BTLA and HVEM. *Nature reviews. Immunology* 6:671-681.
12. Murphy, T.L., and K.M. Murphy. 2010. Slow down and survive: Enigmatic immunoregulation by BTLA and HVEM. *Annual review of immunology* 28:389-411.
13. Sun, Y., N.K. Brown, M.J. Ruddy, M.L. Miller, Y. Lee, Y. Wang, K.M. Murphy, K. Pfeffer, L. Chen, J. Kaye, and Y.X. Fu. 2009. B and T lymphocyte attenuator tempers early infection immunity. *J Immunol* 183:1946-1951.

.

PERSONNEL PAID FROM RESEARCH EFFORT

William E. Gillanders, M.D.

Kenneth Murphy, M.D.

Simon Goedegebuure, Ph.D.

Timothy Fleming, Ph.D.

John Herndon, B.S.

Narendra Sankpal

Xiuli Zhang

Siva Gandhapudi

Teresa L. Murphy, MD

APPENDICES

Appendix #1: Analysis of BTLA expression in human breast cancer

Appendix #2: Establishment of a BALB/c-neuT/BTLA$^{-/-}$ colony for studies of breast cancer immunosurveillance

Appendix #3: Generation and validation of wildtype and mutant HVEM constructs

Appendix #4: Functional analysis of wildtype and mutant HVEM in the context of DNA vaccination

Appendix #5: Establishment and validation of a clinically relevant breast cancer vaccine model

Appendix #6: Defining the role of BTLA in the context of graft-versus-host disease

Appendix #7: Defining the mechanisms of antigen presentation and specific dendritic cell subsets following DNA vaccination

Appendix #8: Targeting murine CD8α+/human CD141+ dendritic cells to transform cancer vaccine therapy

Appendix #1: Analysis of BTLA expression in human breast cancer

To assess the importance of BTLA in human breast cancer, in particular its possible involvement in downregulation of T cell activation, human breast cancers and tumor draining lymph nodes were tested for expression of BTLA by immunohistochemistry and flow cytometry. As follicular helper (CD4) T cells constitutively express BTLA, normal lymph nodes were used to optimize the protocol for BTLA staining of paraffin-embedded tissue. BTLA expression was subsequently assessed in lymph nodes and tumor tissue of patients with breast cancer, both in tissue slides from individual patients and by using a tissue microarray containing >1,000 breast cancer tumors (described in Droeser R et al., *BMC Cancer* 2012, 12:134). Only 1.86% of all cases contained BTLA-positive lymphocytes in the tumor, ranging from 1 to 452 positive lymphocytes.

BTLA positive follicular helper CD4 T cells

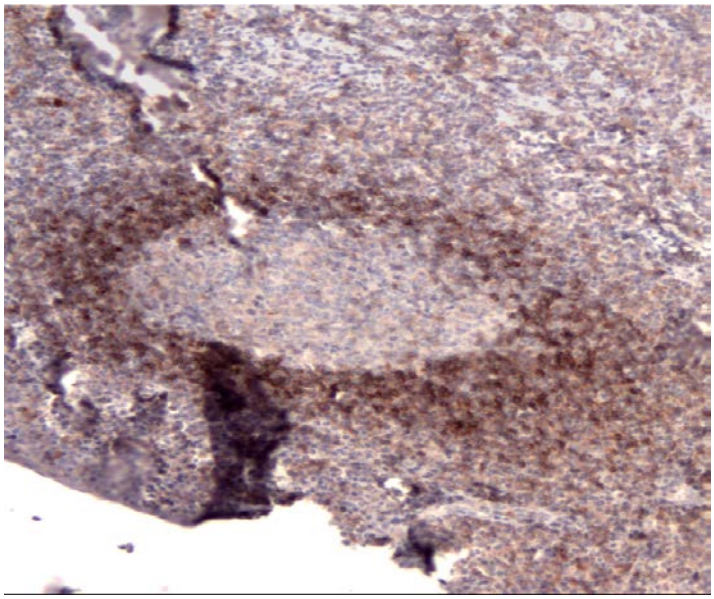

Tumor with BTLA-negative lymphocytes

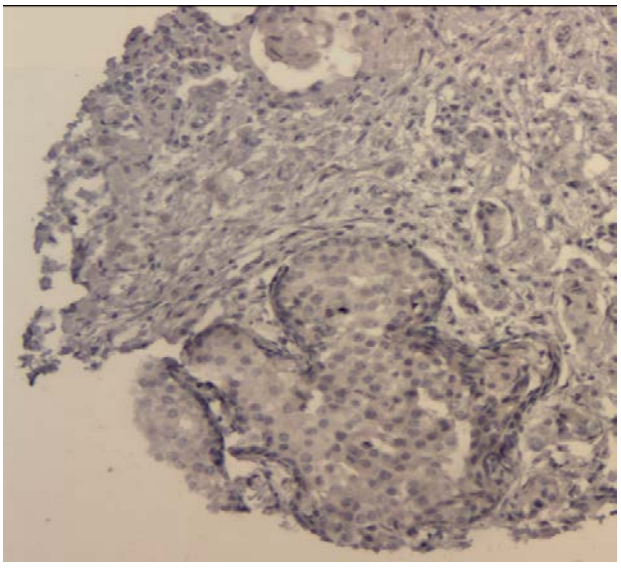

Tumor with a few BTLA-positive lymphocytes

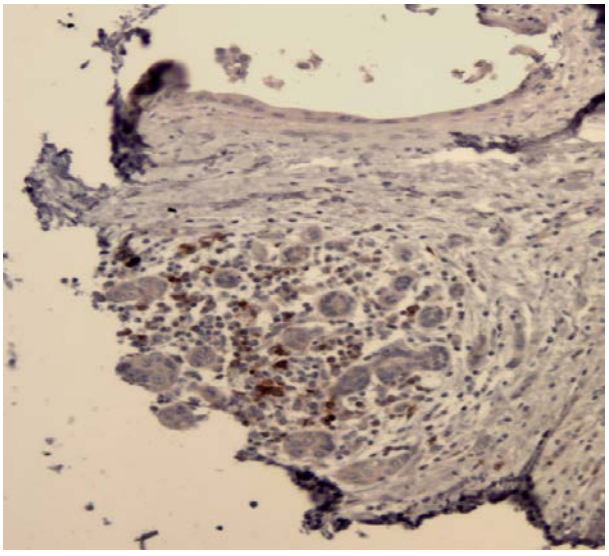

Flow cytometry on single cell suspensions of either freshly obtained lymph nodes or breast tumor tissue was performed in parallel. Cells were stained with antibodies to CD8 and BTLA. Gating on CD8-positive cells was followed by determination of CD8, BTLA double positive cells (see below). Lymph nodes, tumor, and peripheral blood from three patients with confirmed breast cancer were evaluated.

Lymph node

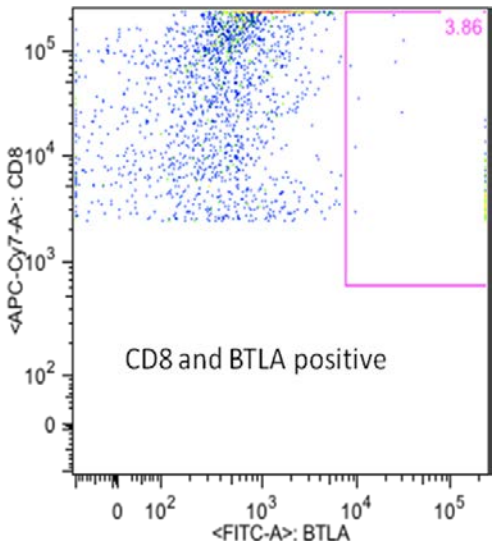

Tumor

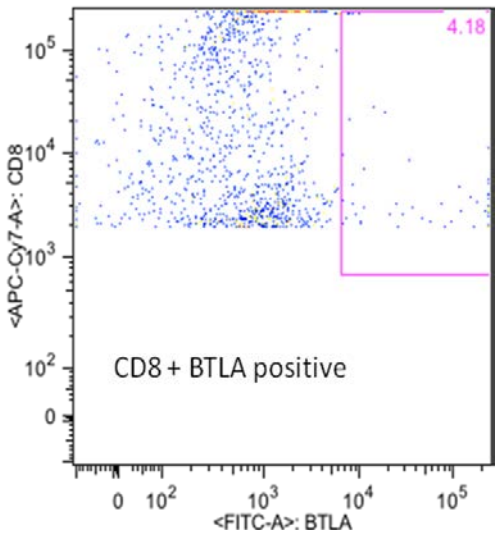

More detailed analysis involving additional lineage and immune subset markers confirmed the low percentage of CD8+BTLA+ lymphocytes in breast cancer patients, but also yielded the surprising finding that a subset of dendritic cells expresses BTLA. This finding was further explored in the context of the recently identified role of this dendritic cell subset in cross-presentation of antigen, and further details are provided in Appendix 4.

In the example below, cells were gated on as follows: live cells, singlets, CD19$^-$, Lin$^-$, HLA-DR$^+$, Clec9a$^+$. Data show 36% of Clec9a$^+$ dendritic cells express BTLA.

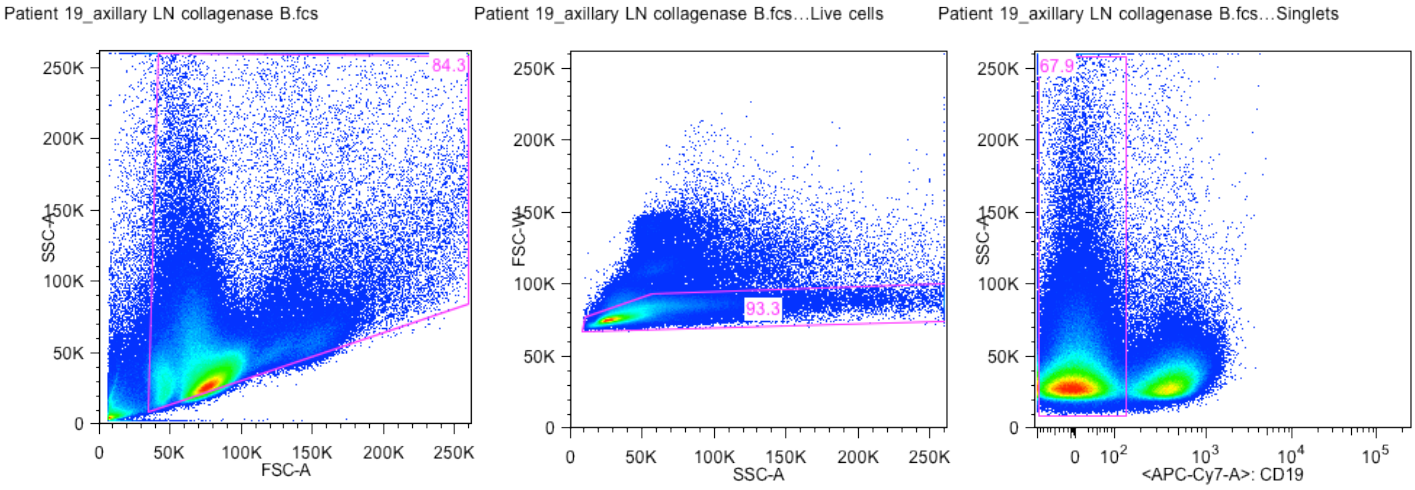

Patient 19_axillary LN collagenase B.fcs…CD19negative

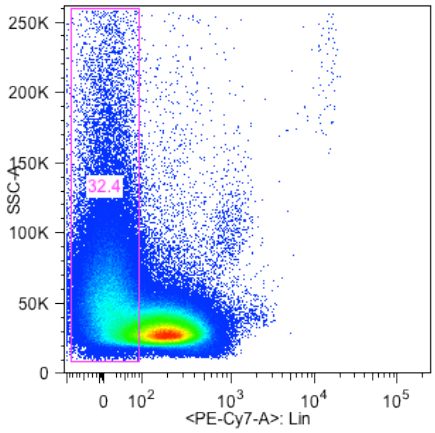

Patient 19_axillary LN collagenase B.fcs…Lin negative

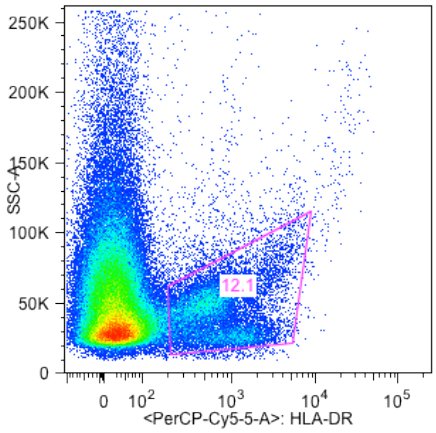

Patient 19_axillary LN collagenase B.fcs…HLA-DR positive

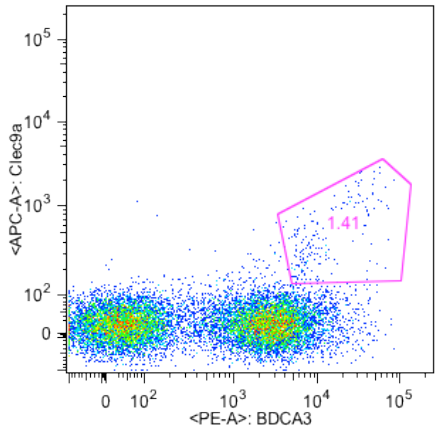

Patient 19_axillary LN collagenase B.fcs…Lymphoid DC

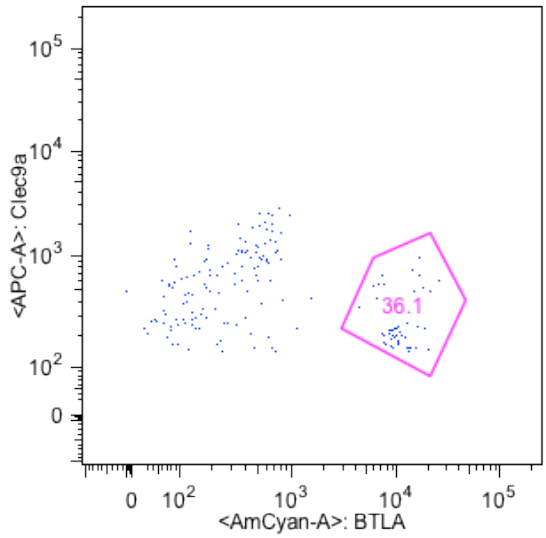

Appendix #2: Establishment of a BALB/c-neuT/BTLA$^{-/-}$ colony

BALB/c-neuT mice were obtained from Eli Gilboa at the University of Miami on two separate occasions. BALB/c-neuT mice from this breeding colony are heterozygous for the neuT transgene, and this remains true in our breeding colony. At each generation, mice must be screened for the presence of the neuT transgene. A PCR-based genotyping reaction was developed to assess for the presence of the neuT transgene (please see below). BTLA-deficient mice on the BALB/c background were generated in the Murphy Laboratory. BALB/c-neuT x BTLA$^{-/-}$ F1 mice are screened for the presence of the neuT transgene. Transgene-positive animals are then backcrossed (F2 generation) to BTLA-/- mice to obtain neuT^{+}, BTLA$^{-/-}$ mice.

PCR Primers for genetyping neuT are: BRL R3 DIR (neu dir): 5'-GTAACACAGGCAGATGTAGGA-3'; MTV RI REV (neu rev): 5'-ATCGGTGATGTCGGCGATAT-3'; β casein (dir): 5'-GATGTGCTCCAGGCTAAAGTT-3'; β casein (rev): 5'-AGAAACGGAATGTTGTGGAGT-3'. Primers to amplify β Casein are used as a positive control, and a no template control is also used (water). The amplification program was performed in a PTC-200 Peltier thermal cycler, and included an initial denaturation at 94°C for 1 min; 35 cycles of 94°C for 1 min, 55°C for 1 min and 72°C for 2 min, and a final incubation at 72°C for 7 min. Each experiment included 5 µL of Bench Top 100 bp DNA ladder (Promega).

Using this protocol, three mice of a BTLA$^{-/-}$ x *neu*T cross were tested, and one was found to be positive for both BTLA-deficiency and expression of *neu*T (lane 2, faint band). We currently are using this mouse as a breeder in order to generate more BTLA$^{-/-}$ x *neu*T mice for future experiments.

β Casein (525 bp)

neuT transgene(230 bp)

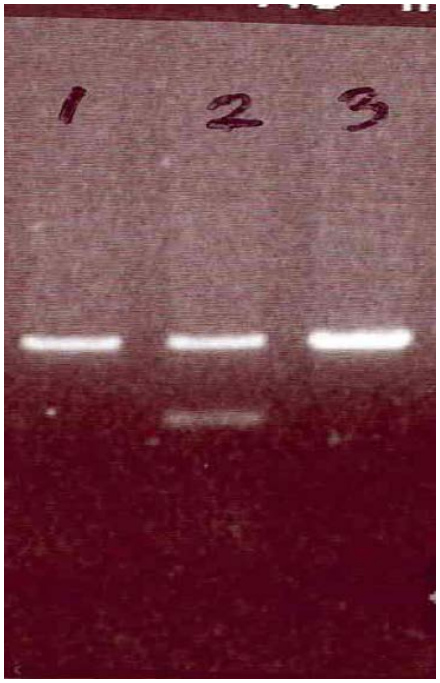

Appendix #3: Generation and validation of wildtype and mutant HVEM constructs

Goal: Introduce three HVEM mutations into the HVEM-IRES-GFP-RV vector (P17A, Y23A, V36A).

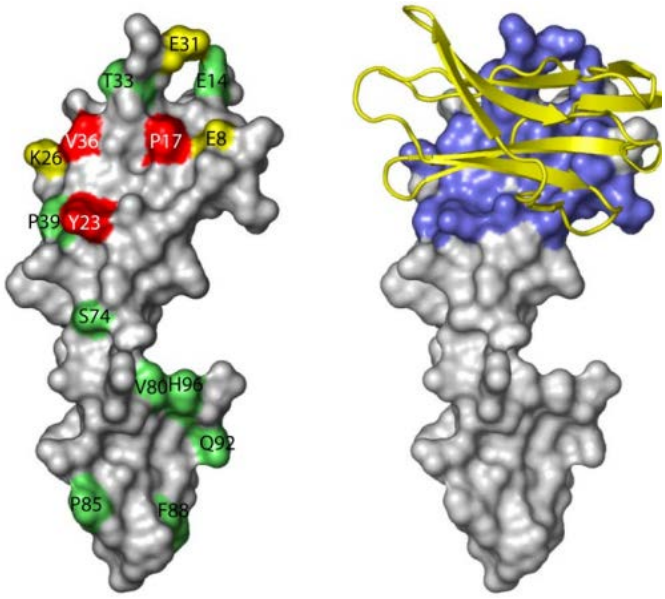

The schematic diagram above shows the position of the HVEM mutants in the HVEM protein. We performed site-directed mutagenesis PCR to amplify HVEM mutants by using HVEM wildtype as a template (HVEM in retroviral vector). Primers used to amplify HVEM mutants (P17A, Y23A, and V36A) are listed below.

Alanine-scanning mutagenesis of HVEM. Mutated residues that reduced BTLA binding > 5-fold (red) are the points we mutated in our HVEM mutants.

HVEM SDM Primers

mP17AFP GACGAGTGCTGCGCCATGTGCAACCCA

mP17ARP TGGGTTGCACATGGCGCAGCACTCGTC

mY23AFP GCAACCCAGGTGCCCATGTGAAGCAGG

mY23ARP CCTGCTTCACATGGGCACCTGGGTTGC

mV36AFP TACAGGCACAGCCTGTGCCCCCTGTCC

mV36ARP GGACAGGGGGCACAGGCTGTGCCTGTA

PCR reactions were performed according to the manufacturer's instructions (Quick-change Lightning Site-Directed Mutagenesis kit from Stratagene). The amplification program was performed in a PTC-200 Peltier thermal cycler, and included an initial denaturation at 95°C for 2 min; 18 cycles of 95°C for 20 sec, 60°C for 10 sec and 68°C for 3 min 30 sec, and a final incubation at 68°C for 5 min. Transformation was performed immediately following PCR. Briefly, 2 µL of DpnI was aliquoted into each vial containing PCR product (50 µL), incubated at 37 °C for 5 min, then 45 µL of XL10 gold ultracompetent cells (XL10G) and 2 µL of β-ME mix were added, and the contents of the tube were swirled gently, and incubated on ice for 2 min. 2 µL of the DpnI-treated DNA from each sample was then transferred to separate aliquots of XL10 G cells, mixed gently and incubated on ice for 30 minutes, followed by a 42 second-heat pulse, then incubated in tubes on ice for 2 minutes. 0.5 mL of preheated NZY+ broth was then added to each tube, and the tubes were incubated at 37°C for 1 hour with shaking at 225-250 rpm. 100 µL of each transformation reaction was then plated on an agar plate containing Amp for the plasmid vector.

The figure below demonstrates the plasmid containing the wildtype and mutant HVEM-IRES-GFP constructs:

HVEM-IRES-GFP-RV (7286 bp)

Constructs were tested by restriction enzyme digest and selected constructs were sent for sequencing to confirm mutations. After confirmation by sequencing, constructs were extracted using a maxi prep kit from Sigma Aldrich.

In order to determine if the wildtype and mutant HVEM constructs can be expressed *in vitro*, we transfected CHO cells with the wildtype and mutant HVEM constructs. GFP expression was assessed using a fluorescence microscope 48 hours after transfection. Subsequently, the transfected CHO cells were stained with HVEM antibody and/or BTLA tetramer followed by flow cytometry. While the wildtype and mutant HVEM constructs in retroviral vectors were prepared in the first year of the award, these key experiments to test construct expression were performed by the new postdoctoral fellow in the second year of the award.

The binding studies demonstrated that binding of BTLA is ablated in the P17A HVEM mutant, whereas binding is intact in the V36A mutant and wildtype HVEM. The Y23A mutation reduced BTLA binding by ~50% (please see below).

Wildtype and mutant HVEM constructs were cloned into retroviral vectors as detailed above. CHO cells were transduced with the indicated constructs, and then stained with PE-conjugated α-HVEM Ab (second row), or PE-conjugated α-BTLA tetramer (third row), and analyzed by flow cytometry. (A) Wildtype and mutant HVEM expression on CHO cells. (B) Summary of FACS staining.

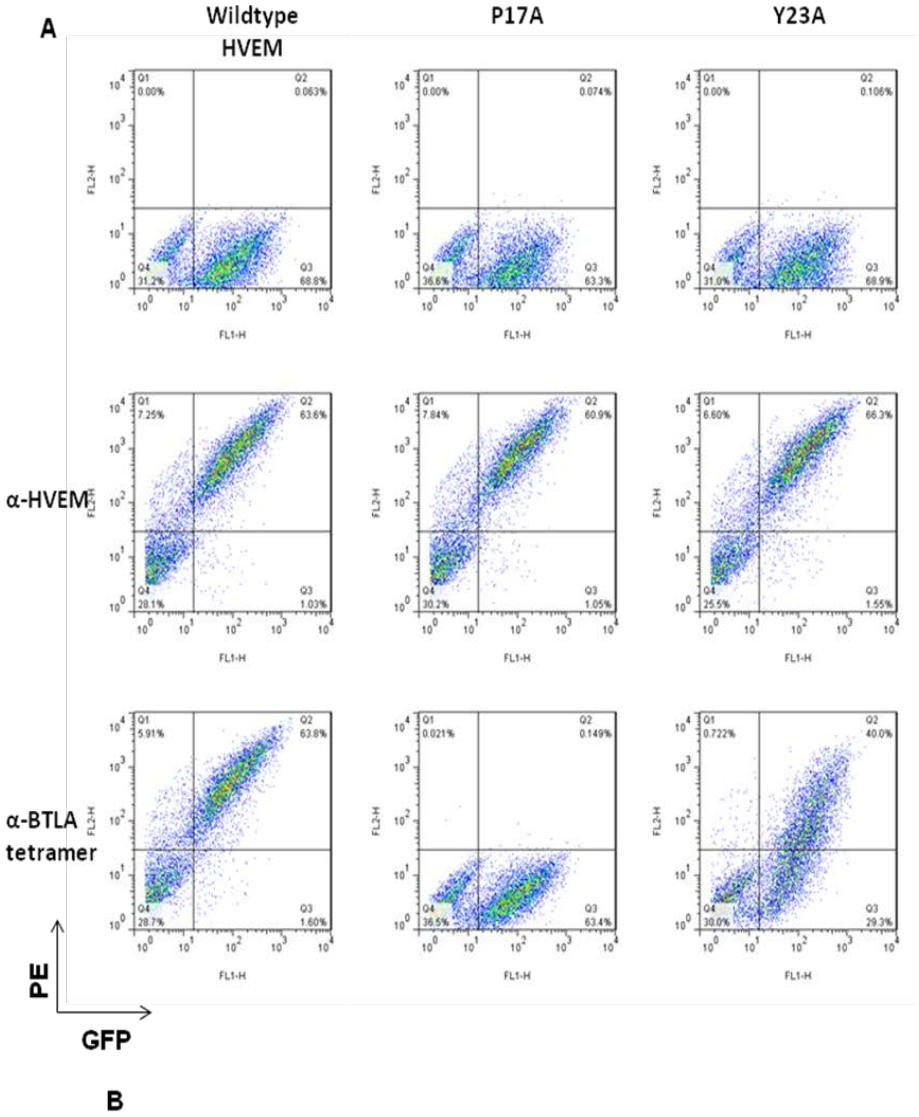

To test the wildtype and mutant HVEM constructs in a DNA vaccine model, the constructs were cloned into the pcDNA3 vector. Two series of constructs were generated, one series with GFP (for *in vitro* studies) and one without GFP (for DNA vaccine studies), and expressed in 293 cells. Flow cytometry was performed to assess expression of GFP and HVEM.

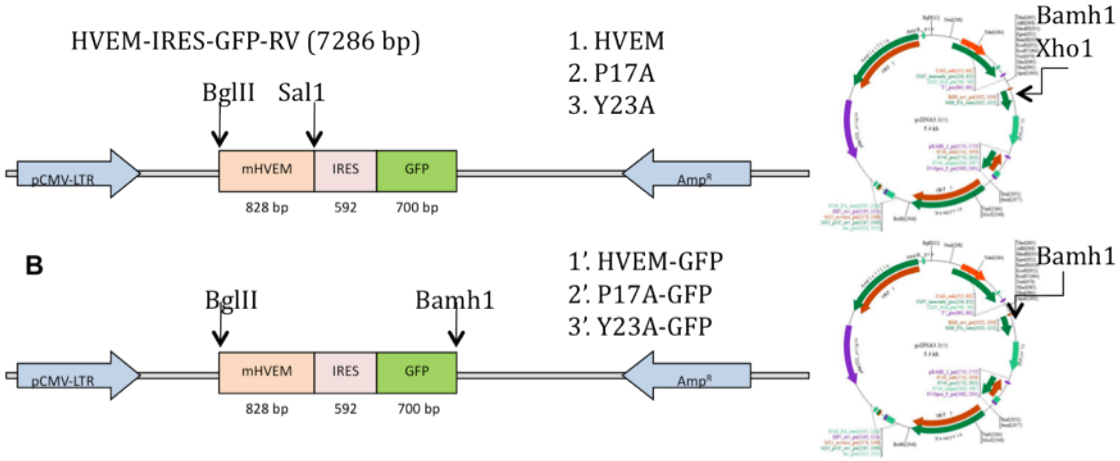

(A, B) Cloning strategy for wildtype and mutant HVEM constructs (P17A, Y23A). All constructs were initially generated by site-directed mutagenesis and cloned into retroviral vectors (shown on left). The constructs were subsequently cloned into pcDNA3 plasmid constructs (shown on right). (A) Wildtype and mutant HVEM constructs were cloned into pcDNA3 without GFP. These constructs are used as molecular adjuvants in DNA vaccine studies. (B) Wildtype and mutant HVEM constructs were cloned into pcDNA3 with GFP for *in vitro* validation studies.

Once the pcDNA3 constructs were validated by restriction digest and sequencing, they were transfected into 293T cells and tested for expression in flow cytometry analyses. Please see below.

(C) Expression of wildtype and mutant HVEM in 293T cells.

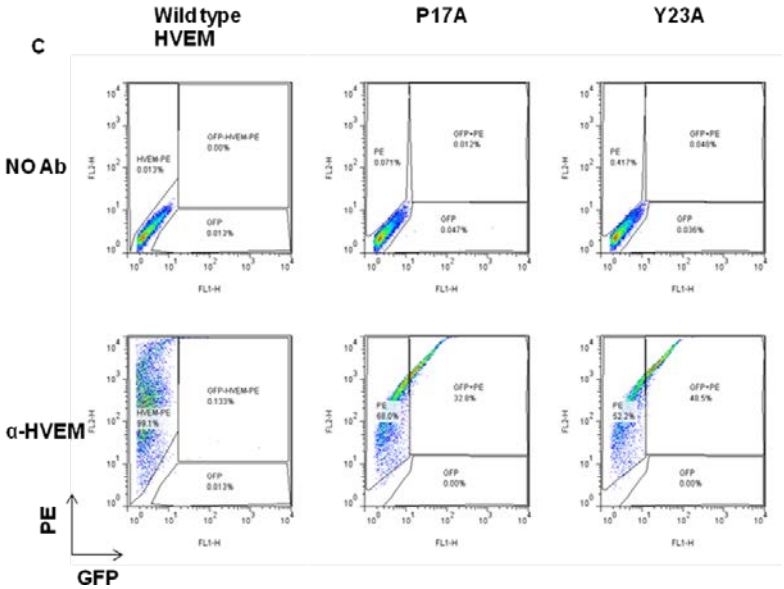

(D) Expression of wildtype and mutant HVEM with GFP in 293T cells. All constructs stain positive for HVEM, but the P17A mutation completely ablates BTLA binding, and the Y23A mutation partially ablates BTLA binding.

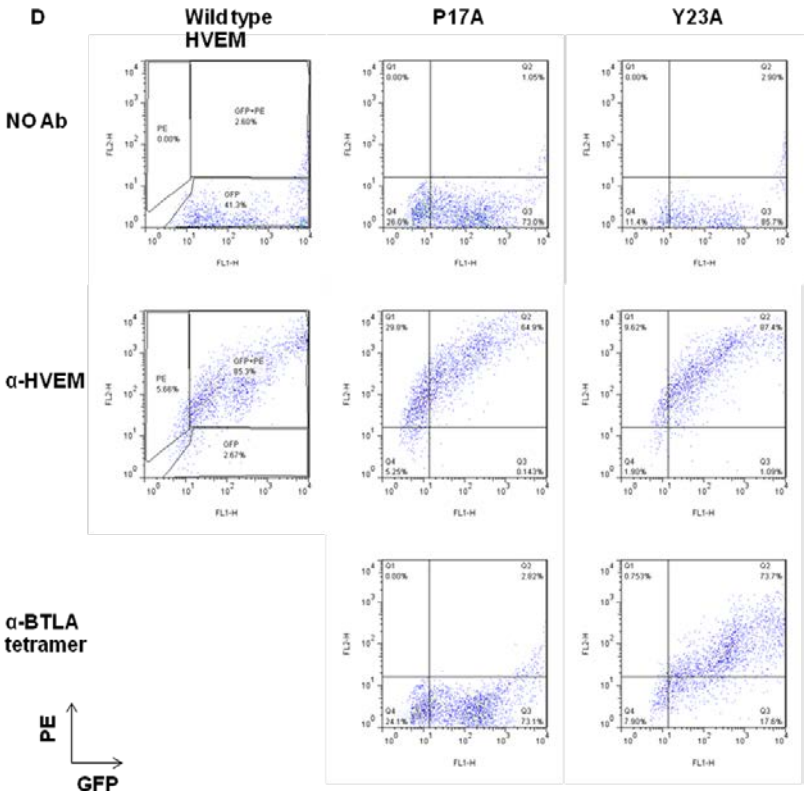

These data show that the wildtype and mutant HVEM constructs are expressed and can be recognized by HVEM-specific antibodies. They also confirm the P17A mutation completely abrogates BTLA binding *in vitro*, whereas the Y23A mutation partially abrogates BTLA binding.

Appendix #4: Functional analysis of wildtype and mutant HVEM in the context of DNA vaccination

To assess if HVEM mutants can enhance the immune response to DNA vaccination, ovalbumin (OVA) cDNA was administered by gene gun with or without wildtype and mutant HVEM constructs. We typically vaccinate mice three times at days 0, 3, and 6, either by gene gun, and assess the primary immune response on day 11 by ELISPOT assay using splenocytes (see below).

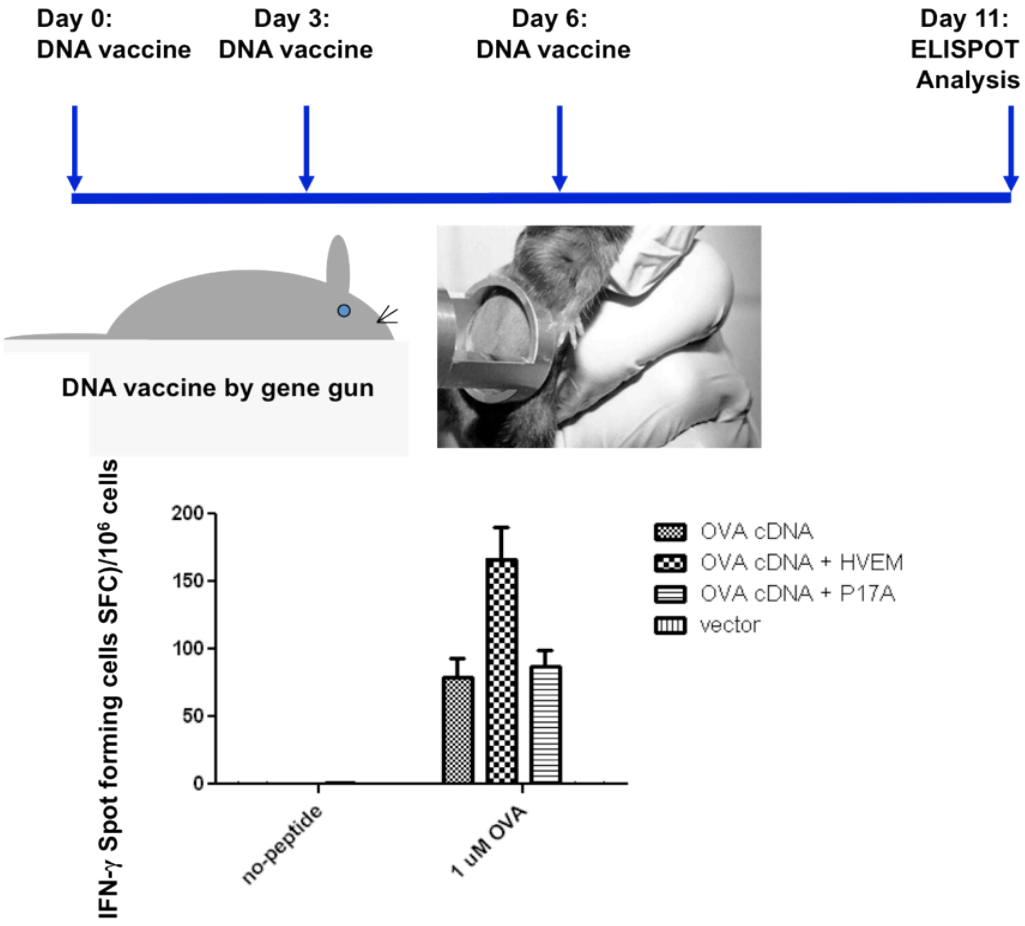

Mice were immunized by gene gun on days 0, day 3 and day 6 with OVA cDNA, OVA cDNA plus HVEM or OVA cDNA plus mutant HVEM P17A. IFN-γ ELISPOT was performed on day 11. Data shown is representative of three independent experiments. Wildtype, but not mutant HVEM enhances the $CD8^+$ T cell response to ovalbumin.

In three independent experiments, administration of wildtype HVEM enhanced the immune response to OVA cDNA. However, unlike wildtype HVEM, the P17A mutant HVEM did not enhance vaccine efficacy.

We performed similar experiments using an electroporation device in a more clinically relevant breast cancer model (see appendix #5 for details on the model). Specifically, we combined wildtype HVEM DNA with breast cancer vaccines, such as neuT cDNA or a single chain trimer DNA vaccine targeting neuT (Kd/Ld SCT).

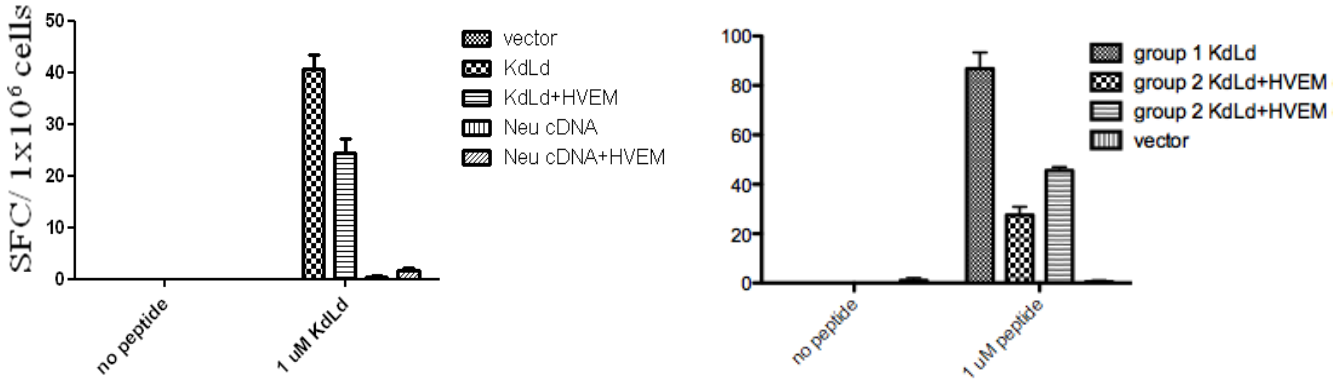

Groups of five BALB/c mice each were vaccinated by electroporation on days 0 and 21. Mice were vaccinated with (1) vector, (2) KdLd SCT DNA, (3) KdLd SCT DNA + wildtype HVEM DNA, (4) neu cDNA, and (5) neu cDNA + wildtype HVEM. One week later, spleens were harvested and splenocytes were tested for recognition of KdLd peptides by IFNγ Elispot. The data represent two independent experiments. *Left panel*: in addition to KdLd SCT DNA, mice were vaccinated with neu cDNA. *Right panel*: HVEM DNA from two separate isolations were tested side-by-side.

The data show that administration of HVEM DNA reduced the immune response unlike in the OVA model. Together these data are confusing and may require more in-depth mechanistic studies on HVEM-BTLA-LIGHT signaling.

Appendix #5: Establishment and validation of a clinically relevant breast cancer vaccine model

While waiting for sufficient numbers of BALB/c-*neu*T mice, we initiated DNA vaccination experiments using the BALB/c mouse breast cancer carcinoma, TUBO. TUBO is a transplantable tumor line that originates from a BALB/c-*neu*T mouse. TUBO expresses neuT, and DNA vaccination against neuT induces TUBO cell rejection. We assessed the efficacy of various neuT DNA vaccines in wild type BALB/c mice challenged with TUBO. In addition to neuT cDNA, we tested two single chain trimer (SCT) constructs expressing immunodominant epitopes of neuT. The SCT DNA constructs encode H-2K^d or H-2L^d, β_2-microglobulin, and the neuT K^d-binding peptide p66-74 (TYVPANASL) or L^d-binding peptide p162-170 (NPQLCYQDM), respectively. Both neuT cDNA and SCT DNA vaccination protected against a lethal challenge of TUBO. The data from the SCT DNA vaccination suggest that neu-specific CD8 T cells were elicited and were capable of rejecting TUBO.

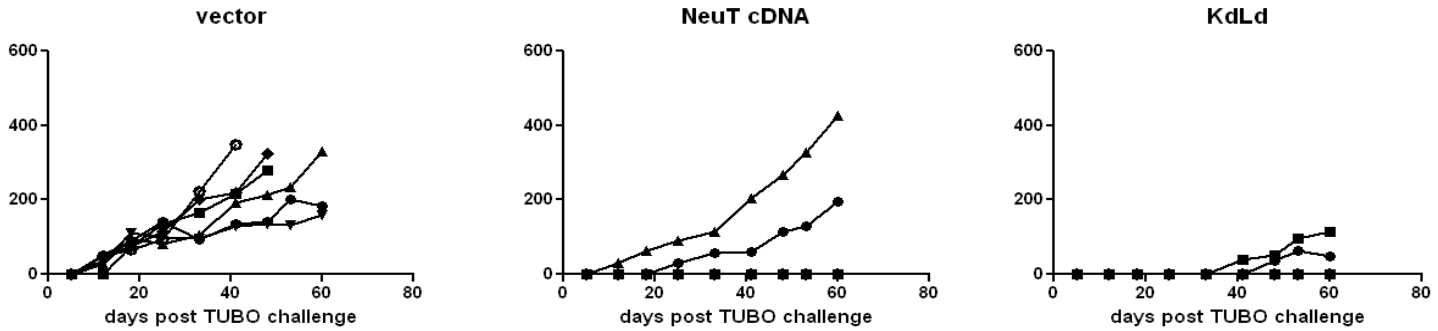

Wild type BALB/c mice (7 per group) were vaccinated on days 0, 3, and 6 by electroporation. On day 37 post immunization, mice were challenged by subcutaneous injection of TUBO (3x105/mouse). Tumor growth was measured every three days using calipers.

To further assess the peptide-specific response elicited by SCT DNA vaccination, ELISPOT assays were performed on splenocytes from vaccinated mice post vaccination.

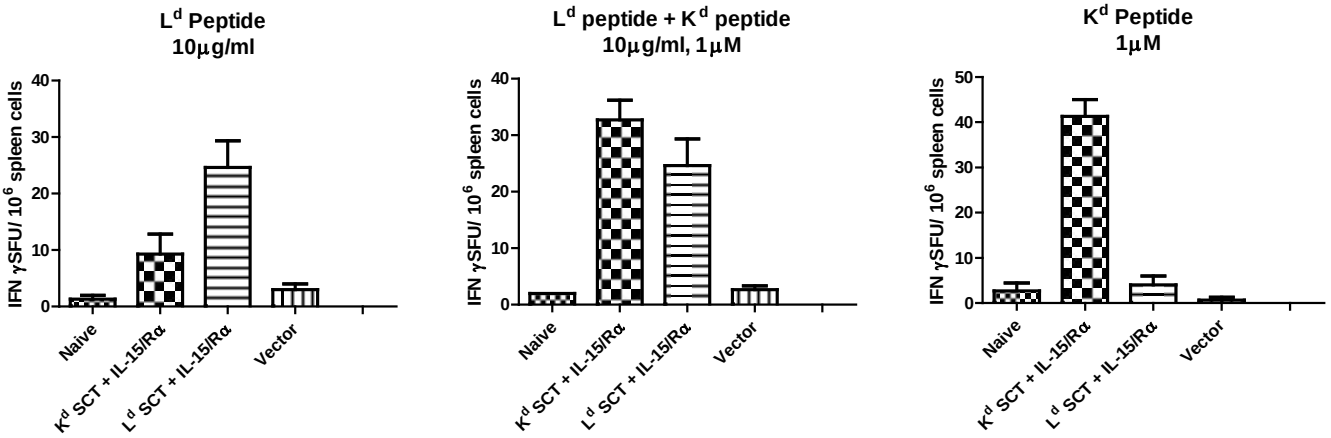

BALB/c mice (3 per group) were vaccinated on days 0, 3, and 6 by electroporation using empty vector DNA or SCT DNA, as indicated plus adjuvant (genetic constructs encoding IL-15 and IL-15Rα). On day 11, ELISPOT assays were performed on isolated splenocytes pulsed with the respective peptides encoded by the SCT constructs.

Appendix #6: Defining the role of BTLA in the context of graft-versus-host disease

Please see the manuscript attached:

Albring, J.C., M.M. Sandau, A.S. Rapaport, B.T. Edelson, A. Satpathy, M. Mashayekhi, S.K. Lathrop, C.S. Hsieh, M. Stelljes, M. Colonna, T.L. Murphy, and K.M. Murphy. 2010. Targeting of B and T lymphocyte associated (BTLA) prevents graft-versus-host disease without global immunosuppression. *The Journal of experimental medicine* 207:2551-2559.

Appendix #7: Defining the mechanisms of antigen presentation and specific dendritic cell subsets following DNA vaccination

Please see the manuscript attached:

Li, L., S. Kim, J.M. Herndon, P. Goedegebuure, T.P. Fleming, T.H. Hansen, K.M. Murphy, and W.E. Gillanders. 2012. Cross-dressed CD8α+ dendritic cells prime CD8+ T cells following vaccination. *Proceedings of the National Academy of Sciences*, 109(31):12716-21.

Appendix #8: Targeting murine CD8α+/human CD141+ dendritic cells to transform cancer vaccine therapy

We have recently made important contributions to the understanding of $CD8^+$ T cell priming, reporting in *Science* a critical role for murine $CD8\alpha^+$ dendritic cells (DC) in priming $CD8^+$ T cell responses to viral infections and cancers [1]. The unique ability of murine $CD8\alpha^+$ DC to prime $CD8^+$ T cells is based in part on their capacity to efficiently cross-present antigen. We and others have recently identified human $CD141^+$ ($BDCA\text{-}3^+$) DC as the lineage and functional equivalent of murine $CD8\alpha^+$ DC, suggesting that our studies of murine $CD8\alpha^+$ DC could be readily translated into the clinic.

In 2008, Dr. Murphy's laboratory reported in the journal *Science* that the transcription factor *Batf3* is critical for the development of $CD8\alpha^+$ DC [1]. *Batf3*$^{-/-}$ mice have a selective loss of $CD8\alpha^+$ and $CD103^+$ DC, without abnormalities in other hematopoietic cell types or architecture. DC from *Batf3*$^{-/-}$ mice are deficient in cross-presentation, and CTL responses to viral infection and syngeneic tumors are impaired in *Batf3*$^{-/-}$ mice [1, 2]. $CD8\alpha^+$ DC appear to be critical for priming anti-tumor $CD8^+$ T cell responses. Wildtype and *Batf3*$^{-/-}$ mice were challenged with syngeneic fibrosarcomas that normally are rapidly rejected in a T cell-dependent manner [3, 4]. Two different fibrosarcomas were rapidly rejected by wildtype mice but grew progressively in *Rag2*$^{-/-}$ mice and *Batf3*$^{-/-}$ mice (Figure 1). Moreover, *Batf3*$^{-/-}$ mice failed to develop tumor-specific $CD8^+$ T cells. Tumor-infiltrating $CD8^+$ T cells, but not $CD4^+$ T cells, were significantly reduced in *Batf3*$^{-/-}$ mice (Figure 2). Likewise, DNA and cellular-based vaccines fail to induce CTL responses in *Batf3*$^{-/-}$ mice. We recently examined the immune response to the model antigen ovalbumin following DNA and/or cellular vaccination in the *Batf3*$^{-/-}$ mouse model. The results are strikingly clear. $CD8^+$ T cell responses were significantly impaired in *Batf3*$^{-/-}$ mice following vaccination, while antibody responses were not impacted (Figure 3 and data not shown). This indicates a near absolute requirement for $CD8\alpha^+$ DC in priming $CD8^+$ T cell responses following vaccination [5].

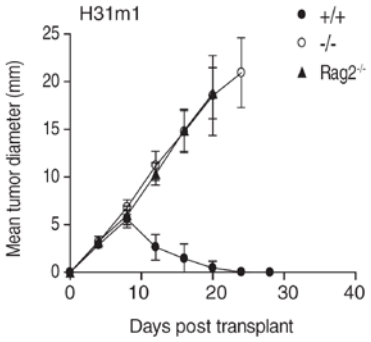

Figure 1. Batf3$^{-/-}$ mice fail to reject syngeneic fibrosarcomas. *1 x 10^6 H31m1 fibrosarcoma cells were injected subcutaneously into wildtype mice (solid circles), Batf3$^{-/-}$ mice (open circles), or Rag2$^{-/-}$ mice (triangles), and tumor diameter was measured (n=10).*

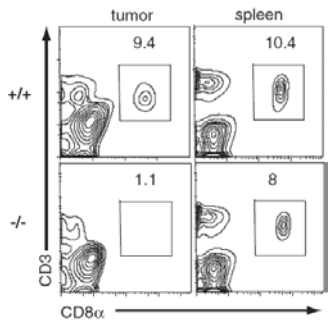

Figure 2. Tumor infiltrating CD8$^+$ T cells are absent in Batf3$^{-/-}$ mice. *Tumors and spleens from mice treated as in Figure 2 were removed on day 11, and analyzed by FACS. Plots are gated on live CD45.2+ cells and show CD3, CD8a, and CD4 expression. Numbers represent the percentage of cells in the indicated gate.*

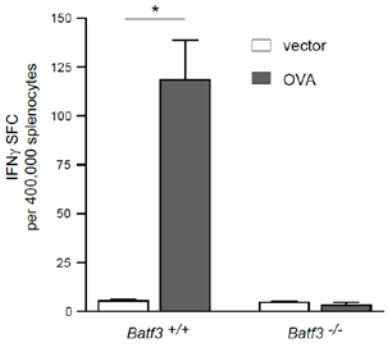

Figure 3. CD8α$^+$ DC are required for induction of CD8$^+$ T cells by DNA vaccines. *ELISPOT for interferon-γ (IFNγ) production by CD8 T cells from wildtype (Batf3$^{+/+}$) or Batf3$^{-/-}$ mice immunized with an ovalbumin-expressing DNA vaccine (OVA) or empty vector (vector).*

CD8α$^+$ DC express very high BTLA and may activate HVEM signaling in CD8$^+$ T cells. Dr. Murphy's laboratory discovered BTLA [6] and identified its ligand HVEM [18]. Although BTLA was initially described as a T cell co-inhibitory molecule, we have now demonstrated that signaling in the BTLA-HVEM costimulatory system is bidirectional [7-12], and the overall impact of BTLA expression on immune responses has not been fully elucidated. In preliminary studies we focused on targeting the BTLA-HVEM-LIGHT costimulatory system to enhance vaccine efficacy. We demonstrated that HVEM can be used as a molecular adjuvant in DNA vaccination, providing important proof-of principle that BTLA can be successfully targeted. These studies prompted us to measure BTLA expression by CD8α$^+$ DC, and we have now made the surprising finding that murine CD8α$^+$ DC express the highest levels of BTLA of any immune cell, much higher than B cells and other types of DC (Figure 4). This could provide CD8α$^+$ DC with the unique ability to strongly activate CD8$^+$ T cells via HVEM. We know that HVEM is important for CD8$^+$ T cell responses against *Listeria monocytogenes* [13]. In collaboration, we have now demonstrated that HVEM is required for CD8$^+$ T cell memory following vaccinia infection (submitted), suggesting costimulation via BTLA on CD8α$^+$ DC may be required. We will further test the importance of BTLA expression by CD8α$^+$ DC in the CD8$^+$ T cell response to vaccination. Of note, we have extended our studies to human CD141$^+$ DC, demonstrating that this subtype also expresses BTLA at very high levels (Figure 5).

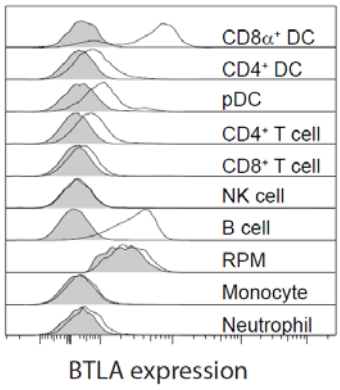

Figure 4. CD8α$^+$ DCs express the highest level of BTLA of any immune cell type. *The indicated subsets of murine myeloid and lymphoid cells were identified by various markers. Shown is BTLA expression as a single color histogram for the indicated lineage.*

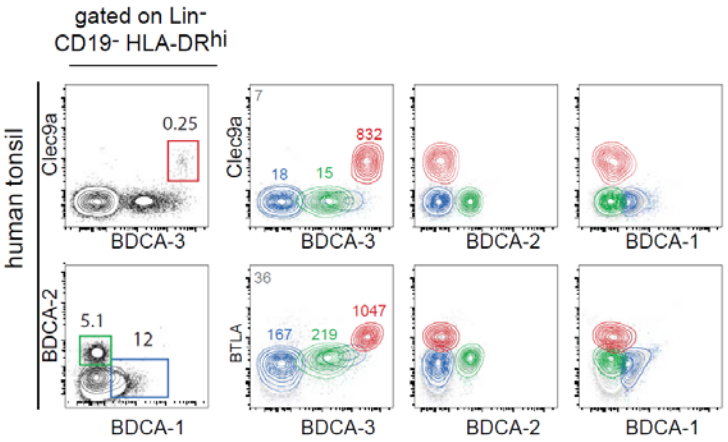

Figure 5. Human CD141$^+$ DC express BTLA. *Human tonsil was stained for expression of CD19, HLA-DR, CLEC9a, BDCA-1, BDCA-2, BDCA-3 and BTLA. Cells in the indicated gates (left column) are shown as color-coded two-color histograms on the right for the indicated surface markers. Results show that theCD141$^+$ (Clec9a$^+$/BDCA-3$^+$) DC (red) are uniformly high for BTLA expression relative to the BDCA-2$^+$ pDC (green) and BDCA-1$^+$ cDC (blue). Numbers indicate the mean fluorescence index (MFI) of the cells in the indicated gates.*

This work is currently being written for publication as brief definitive report to be submitted to the Journal of Experimental Medicine. More importantly, we (Drs. Gillanders and Murphy) were recently successful in securing funds to continue this exciting research.

Published November 15, 2010

Targeting of B and T lymphocyte associated (BTLA) prevents graft-versus-host disease without global immunosuppression

Jörn C. Albring,[1,2] Michelle M. Sandau,[1] Aaron S. Rapaport,[1] Brian T. Edelson,[1] Ansuman Satpathy,[1] Mona Mashayekhi,[1] Stephanie K. Lathrop,[3] Chyi-Song Hsieh,[3] Matthias Stelljes,[4] Marco Colonna,[1] Theresa L. Murphy,[1] and Kenneth M. Murphy[1,2]

[1]Department of Pathology and Immunology, [2]Howard Hughes Medical Institute, and [3]Department of Medicine, Division of Rheumatology, Washington University School of Medicine, St. Louis, MO 63110
[4]Department of Medicine/Hematology and Oncology, University of Muenster, 48149 Muenster, Germany

Graft-versus-host disease (GVHD) causes significant morbidity and mortality in allogeneic hematopoietic stem cell transplantation (aHSCT), preventing its broader application to non–life-threatening diseases. We show that a single administration of a nondepleting monoclonal antibody specific for the coinhibitory immunoglobulin receptor, B and T lymphocyte associated (BTLA), permanently prevented GVHD when administered at the time of aHSCT. Once GVHD was established, anti-BTLA treatment was unable to reverse disease, suggesting that its mechanism occurs early after aHSCT. Anti-BTLA treatment prevented GVHD independently of its ligand, the costimulatory tumor necrosis factor receptor herpesvirus entry mediator (HVEM), and required BTLA expression by donor-derived T cells. Furthermore, anti-BTLA treatment led to the relative inhibition of $CD4^+$ forkhead box $P3^-$ ($Foxp3^-$) effector T cell (T eff cell) expansion compared with precommitted naturally occurring donor-derived $CD4^+$ $Foxp3^+$ regulatory T cell (T reg cell) and allowed for graft-versus-tumor (GVT) effects as well as robust responses to pathogens. These results suggest that BTLA agonism rebalances T cell expansion in lymphopenic hosts after aHSCT, thereby preventing GVHD without global immunosuppression. Thus, targeting BTLA with a monoclonal antibody at the initiation of aHSCT therapy might reduce limitations imposed by histocompatibility and allow broader application to treatment of non–life-threatening diseases.

CORRESPONDENCE
Kenneth M. Murphy:
kmurphy@wustl.edu

Abbreviations used: aHSCT, allogeneic hematopoietic stem cell transplantation; BLI, bioluminescence imaging; BMC, BM cell; BTLA, B and T lymphocyte associated; Foxp3, forkhead box P3; GVHD, graft-versus-host disease; GVT, graft versus tumor; HVEM, herpesvirus entry mediator; MCMV, murine CMV; TCD-BM, T cell–depleted BMC; T eff cell, $CD4^+Foxp3-$ effector T cell; T reg cell, $CD4^+Foxp3^+$ regulatory T cell.

Replacement of an abnormal lymphohematopoietic system by allogeneic hematopoietic stem cell transplantation (aHSCT) from a healthy donor is an effective treatment for many disorders of the hematopoietic system (Sykes and Nikolic, 2005; Copelan, 2006). Induction of a mixed hematopoietic donor-host chimerism can induce long-lasting tolerance to foreign tissues without the need for life-long immunosuppressive therapy (Kawai et al., 2008). aHSCT therapy has been improved by better donor identification (Petersdorf et al., 2004), more tolerable conditioning regimens (McSweeney et al., 2001), and enhanced supportive care. However, significant treatment-related morbidity and mortality from chemotherapy, radiotherapy, infections, and graft-versus-host disease (GVHD) remain significant clinical problems. Therefore, aHSCT is commonly indicated only for treatment of conditions where other treatment options are far inferior or lacking.

Costimulatory molecules of the CD28 and TNF families regulate GVHD, with inhibitory and activating receptors either decreasing or increasing its severity (Tamada et al., 2000; Blazar et al., 2003; Xu et al., 2007). B and T lymphocyte associated (BTLA) is an inhibitory immunoglobulin superfamily receptor, whose ligand is the TNF receptor herpesvirus entry mediator

J.C. Albring and M.M. Sandau contributed equally to this paper.

The Rockefeller University Press $30.00
J. Exp. Med. Vol. 207 No. 12 2551-2559
www.jem.org/cgi/doi/10.1084/jem.20102017

Supplemental Material can be found at:
http://jem.rupress.org/content/suppl/2010/11/12/jem.20102017.DC1.html

Published November 15, 2010

(HVEM) and which has only been examined in a nonirradiated model of chronic allostimulation without classical GVHD where donor cells lacking BTLA failed to persist (Hurchla et al., 2007). The role of BTLA in aHSCT using irradiated recipients, in which clinical symptoms and pathology similar to human GVHD develop, has not been examined.

RESULTS AND DISCUSSION

To determine the role of BTLA in the development of GVHD, we first examined WT and BTLA$^{-/-}$ donor mice (Watanabe et al., 2003) using a nonlethal parent-into-irradiated F1 model of aHSCT (Stelljes et al., 2008). In this model, GVHD results from partial MHC mismatch between H-2^{b} haplotype donor cells and lethally irradiated H-2$^{b/d}$ haplotype recipients. BM and splenocytes from WT or BTLA$^{-/-}$ mice on the C57BL/6 background were transferred into lethally irradiated CB6F1 recipients (Fig. 1 a). Transplantation of WT donor cells into CB6F1 recipients caused body weight loss of ~30% and clinical scores (Cooke et al., 1996) of ~3 that persisted for >40 d. BTLA$^{-/-}$ and WT donor cells caused similar GVHD, suggesting that BTLA does not normally regulate GVHD in this model. To test whether BTLA expressed by recipient mice might regulate GVHD in this model, we used BTLA$^{-/-}$ CB6F1 hosts as recipients of BTLA$^{-/-}$ BM and splenocytes (Fig. S1 a). BTLA$^{-/-}$ donor cells induced similar GVHD in BTLA$^{+/-}$ and BTLA$^{-/-}$ hosts, which is comparable to GVHD by WT donor cells (Fig. 1 a). Collectively, these data suggest that BTLA does not normally regulate GVHD.

Because BTLA generates inhibitory signals and functions in autoimmunity (Watanabe et al., 2003), malaria infection (Lepenies et al., 2007), and intestinal inflammation (Steinberg et al., 2008), we wondered whether harnessing the inhibitory effects of BTLA on the immune response by forced engagement would attenuate GVHD. To test this, we compared the effects of an agonistic nondepleting anti-BTLA monoclonal antibody (Hurchla et al., 2005; Lepenies et al., 2007), 6A6, administered at the time of aHSCT (Fig. 1 b) with an isotype control antibody, PIP, that recognizes bacterial GST (Gronowski et al., 1999). Mice treated with PIP showed similar progression of GVHD (Fig. 1, a and b), with clinical scores between 3 and 4 persisting for >140 d (Fig. S1 b). GVHD was associated with thickening of the lamina propria and muscularis, with severe inflammation and ulceration of

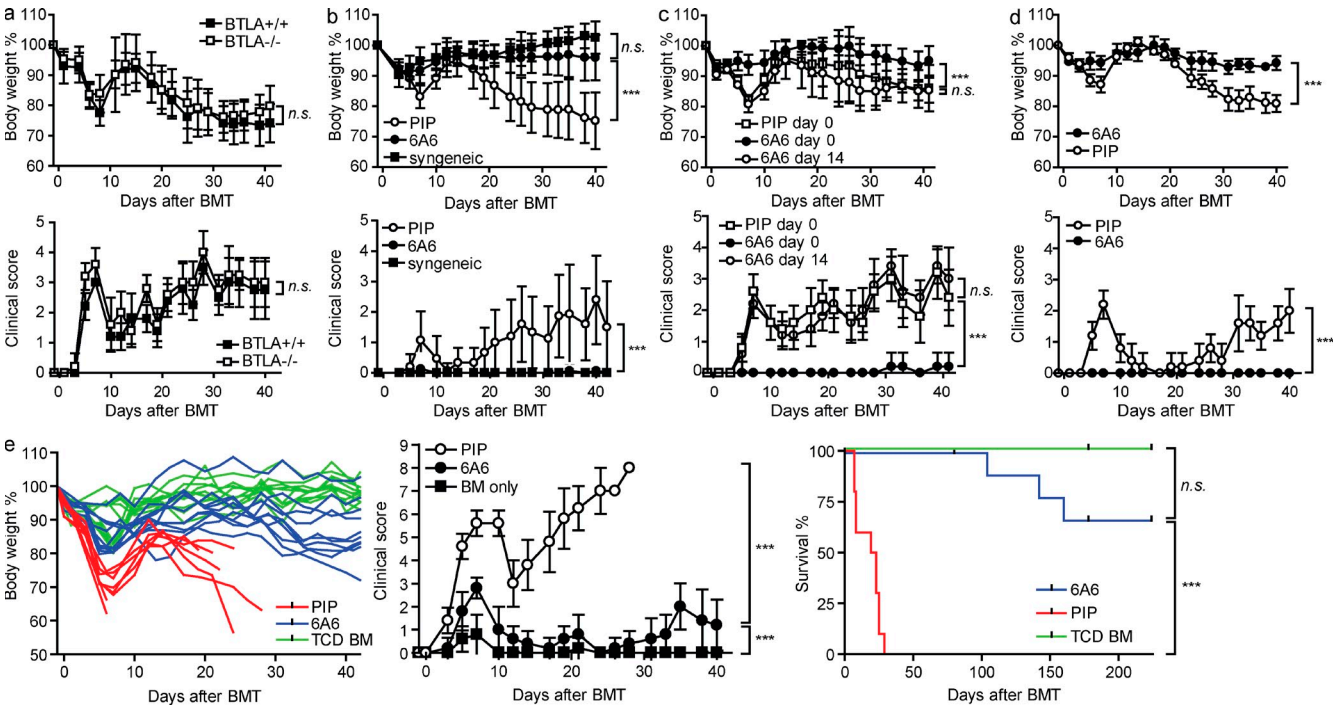

Figure 1. Anti-BTLA treatment permanently prevents GVHD. (a) Lethally irradiated CB6F1 mice received BMC and splenocytes from C57BL/6 WT (closed squares, $n = 5$) or BTLA$^{-/-}$ (open squares, $n = 5$) donors. (b) Lethally irradiated CB6F1 mice received BMC and splenocytes from syngeneic donors (closed squares, $n = 10$), C57BL/6 mice and antibodies PIP (open circles, $n = 15$), or 6A6 (closed circles, $n = 15$). Shown are cumulative data from three independent experiments. (c) Lethally irradiated CB6F1 mice received BMC and splenocytes from C57BL/6 mice plus control antibody PIP (open circles, $n = 5$) or 6A6 (closed circles, $n = 5$) on the day of BMT or 6A6 14 d after BMT (open squares, $n = 5$). (d) Lethally irradiated CB6F1 mice received BMC and splenocytes from C57BL/6 HVEM$^{-/-}$ mice and control antibody PIP (open circles, $n = 5$) or 6A6 (closed circles, $n = 5$). (e) Lethally irradiated BALB/c mice received TCD-BM alone (green lines and closed squares, $n = 10$) or in combination with splenocytes from C57BL/6 mice and control antibody PIP (red lines and open circles, $n = 10$) or 6A6 (blue lines and closed circles, $n = 10$) on the day of BMT. Shown are cumulative data from two independent experiments. Weight and clinical score data shown are mean ± SD. Data are representative of two independent experiments with five mice per group or cumulative data from independent experiments as indicated. P-values of >0.05 are considered not significant (n.s). ***, $P < 0.001$.

Published November 15, 2010

the colon (Stelljes et al., 2008; Fig. S1 c, bottom). In contrast, a single treatment of 10 μg/g body weight of 6A6, given at the time of aHSCT, prevented GVHD completely, with weight loss and GVHD similar to the syngeneic control group (Fig. 1 b) for 140 d after aHSCT (Fig. S1 b). Furthermore, 6A6-treated mice had no histological evidence of GVHD in the colon (Fig. S1 c, top). Thus, a single administration of anti-BTLA antibody eliminates weight loss, histological changes, and clinical signs of GVHD.

We next asked if 6A6 acted by simply depleting donor cells that express BTLA. As a positive control, we included a depleting murine anti-BTLA antibody, 6F7 (Hurchla et al., 2005; Truong et al., 2009). CFSE-labeled donor cells were transferred into WT recipients that also received PIP, 6A6, or 6F7 antibody. 2 d after transfer, we found similar numbers of $CFSE^+$ cells in mice that received either PIP or 6A6 antibody (Fig. S1 d, left) and no significant differences between numbers of $CD19^+$, $CD4^+$, or $CD8^+$ lymphocytes (Fig. S1 d, right). Treatment with 6F7 caused a significant depletion of $CFSE^+$ lymphocytes, particularly from the $CD19^+$ cell population (Fig. S1 d). Furthermore, surface-bound 6A6 was detectable on live donor-derived cells in vivo up to 7 d after transfer (Fig. S1 e). In addition, 6A6 treatment was unable to prevent GVHD caused when $BTLA^{-/-}$ donors were used as a source of BM for aHSCT (Fig. S1 f). Thus, 6A6 does not deplete lymphocytes (Hurchla et al., 2007; Lepenies et al., 2007) but requires the expression of BTLA on donor cells to prevent GVHD.

Next, we asked if 6A6 could reverse established GVHD. We compared immediate with delayed administration of 6A6 (Fig. 1 c). Again, immediate 6A6 administration prevented GVHD. In contrast, there was no statistical difference in weight loss or clinical scores between mice that received 6A6 14 d after aHSCT and with mice that received PIP (Fig. 1 c).

6A6 binds to a region of BTLA that is involved in interactions with HVEM (Hurchla et al., 2005). Thus, 6A6 might prevent GVHD by preventing HVEM and BTLA interactions, thus blocking costimulatory signaling to donor cells (Xu et al., 2007). Although our data indicated that host BTLA is not involved (Fig. S1 a), we wished to test this possibility independently. Transfer of $HVEM^{-/-}$ donor cells caused induction of GVHD when administered with PIP (Fig. 1 d). The severity of GVHD caused by $HVEM^{-/-}$ donor cells was somewhat less than that caused by WT donor cells (Fig. 1 b), consistent with a study which found that HVEM and LIGHT are costimulatory in promoting GVHD (Xu et al., 2007). However, 6A6 also prevented GVHD caused by $HVEM^{-/-}$ donor cells (Fig. 1 d). These results indicate that 6A6 prevents GVHD in a manner that is independent of HVEM, suggesting it acts directly through BTLA.

Because the parent-into-irradiated F1 model of aHSCT does not result in lethal GVHD, we wished to test the potency of the anti-BTLA treatment in a model of complete MHC mismatch ($H\text{-}2^b$ into $H\text{-}2^d$) that results in lethal GVHD in untreated mice (Lu et al., 2001; Edinger et al., 2003b). Control mice developed severe GVHD with pronounced weight loss and clinical scores of >6 (Fig. 1 e, left and middle) and died within 30 d after aHSCT from severe GVHD (Fig. 1 e, right). Although mice that received the anti-BTLA treatment were not fully protected from GVHD, with clinical scores ranging from 1 to 3 (Fig. 1 e, middle) and slightly more weight loss than the control group that had received T cell–depleted BM cells (BMCs [TCD-BMs]) alone (Fig. 1 e, left), 70% of recipients treated with 6A6 survived for >200 d after aHSCT.

Although the precise molecular targets of BTLA signaling are still obscure (Gavrieli and Murphy, 2006; Wu et al., 2007), BTLA engagement by HVEM can inhibit T cell proliferation in vitro (Sedy et al., 2005) and promote tolerance induction in vivo (Liu et al., 2009). Therefore, we asked if anti-BTLA treatment alters donor T cell proliferation or IL-2 production in vivo. CFSE-labeled donor splenocytes were transferred into CB6F1 recipients that were treated with PIP, 6A6, or 6F7. Donor T cell proliferation was assessed after aHSCT and, by 3 d after aHSCT, reduced CFSE levels suggested that proliferation had occurred (Fig. 2 e). $CD4^+$ T cells had reduced proliferation after treatment with 6A6 and 6F7 antibodies 3 d after aHSCT (Fig. 2 e, middle), and the total accumulation of donor $CD4^+$ T cells was significantly reduced compared with control ($P < 0.0018$ and $P < 0.0083$; Fig. 2 b). In contrast, $CD8^+$ T cell proliferation and accumulation were not significantly affected by 6A6 treatment ($P < 0.8489$; Fig. 2, a and e, left). As 6F7 treatment leads to partial depletion of cells, we also assessed the level of annexin V binding, which is an indicator of early apoptosis. Mice treated with 6F7, but not PIP or 6A6, showed increased binding of annexin V on $CD4^+$ and $CD8^+$ T cells 7 d after aHSCT, which was not observed on day 3 (Fig. S1 g).

Although accumulation of $CD4^+$ T cells was lower in 6A6-treated than in PIP-treated mice, the production of IL-2 7 d after aHSCT was not statistically different (Fig. S2, a and b). A small but significant reduction in IFN-γ and IL-4, but not IL-17, production was observed in 6A6-treated mice compared with controls (Fig. S2, a and b). In summary, 6A6 administered at the time of aHSCT reduced the proliferation and accumulation of donor-derived $CD4^+Foxp3^-$ effector T cells (T eff cells) without inducing anergy, inhibiting IL-2 production or causing major alterations in cytokines.

These effects were suggestive of the actions of $CD4^+$ $Foxp3^+$ regulatory T cells (T reg cells) expressing the transcription factor forkhead box P3 (Foxp3; Hori et al., 2003). T reg cells have recently been reported to play a significant role in regulating GVHD (Taylor et al., 2002; Edinger et al., 2003b), and there are ongoing clinical trials aimed directly at the use of T reg cells as an intervention in human GVHD (NCI clinical trial NCT00725062).

To determine whether 6A6 treatment influences T reg cells, we measured the accumulation and proliferation of donor-derived T eff cells after aHSCT (Fig. 2, c and e, right). In PIP-treated recipients that developed GVHD, significantly fewer T reg cell were detected 7 d ($P < 0.0393$) after aHSCT when compared with recipients that received either anti-BTLA treatment 6A6 or 6F7 (Fig. 2 c). Therefore, anti-BTLA treatment inhibits the proliferation of T eff cells yet

Published November 15, 2010

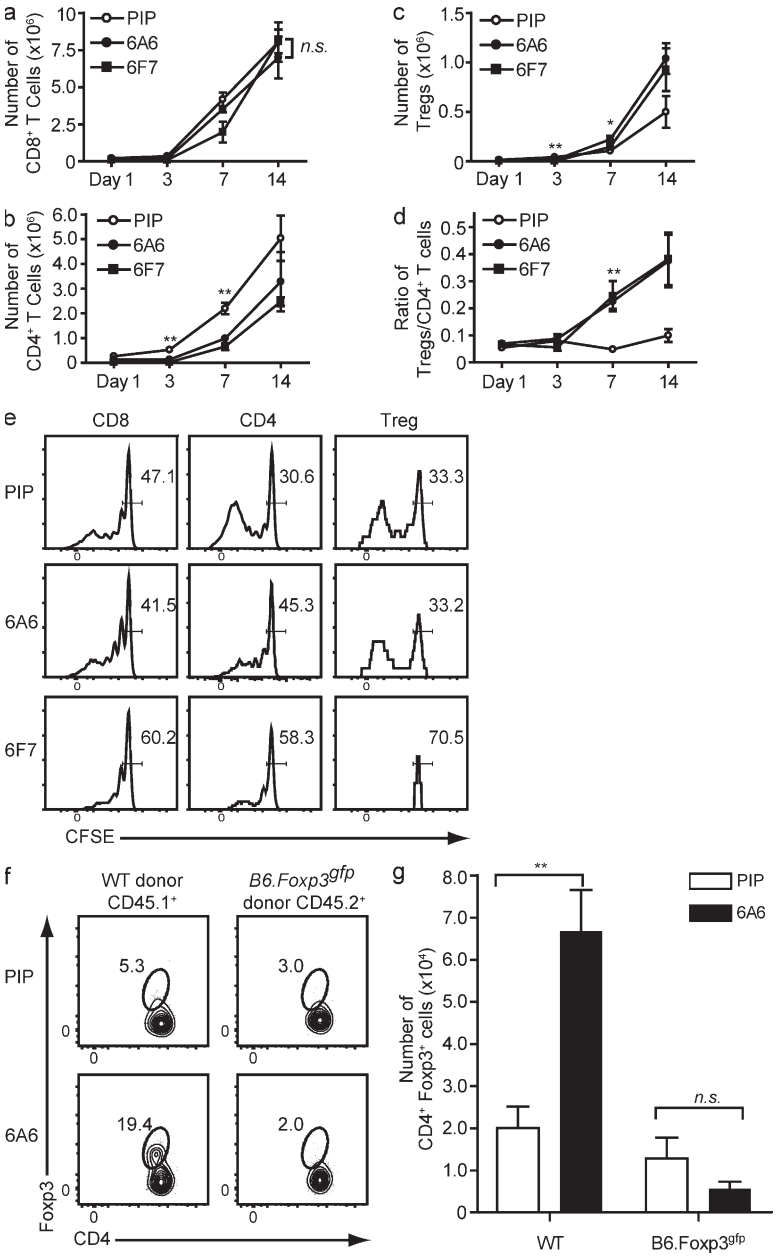

Figure 2. Anti-BTLA treatment allows for the expansion of preexisting donor-derived T reg cells by inhibiting T eff cell proliferation. (a–e) Lethally irradiated CB6F1 mice received a CFSE-labeled graft from B6.SJL donors and were treated with control antibody PIP (open circles), 6A6 (closed circles), or 6F7 (closed squares; $n = 3$ per group). The number of CD8+ T cells (a), CD4+Foxp3− (b), and CD4+ Foxp3+ (c) was calculated from absolute numbers of live splenocytes, and the percentage of the lymphocyte population was assayed by flow cytometry. (d) The ratio of total CD4+Foxp3+/CD4+Foxp3− cells was calculated at the indicated time points by dividing the number of T reg cells in c by the number of T eff cells in b. (e) CFSE intensity of CD8+, CD4+Foxp3−, and CD4+Foxp3+, 3 d after aHSCT with PIP, 6A6, or 6F7 treatment. (f and g) Lethally irradiated CB6F1 mice received aHSCT from B6.SJL mice along with purified CD4+ Foxp3-negative T cells from *B6.Foxp3^{gfp}* mice with control antibody (PIP) or 6A6 ($n = 5$ per group). After 7 d, splenocytes were assayed by flow cytometry to determine the relative frequency of CD4+Foxp3+ cells among CD4+ cells (f) or the absolute number of CD4+Foxp3+ T reg cells (g). Statistical comparisons in a–d are between the PIP- and 6A6-treated groups at the indicated time point, and the data are displayed as mean ± SEM. Shown are representative data from two independent experiments with three to five mice per group. P-values of >0.05 are considered not significant (n.s). *, 0.01 < P < 0.05; **, 0.001 < P < 0.01.

allows the accumulation of T reg cells, resulting in an increased T reg/T eff cell ratio ($P > 0.0028$; Fig. 2 d). This result is in agreement with the demonstration that T reg cells maintain low levels of BTLA after activation, in contrast to conventional T cells which up-regulate BTLA expression upon activation (Fig. S2 c; Hurchla et al., 2005). Thus, 6A6 treatment increases the numbers and the frequency of donor-derived T reg cells after aHSCT.

6A6 treatment could increase T reg cell frequency either by inducing Foxp3 expression in naive donor CD4+ T cells (Chen et al., 2003) or by causing in vivo expansion of preexisting donor T reg cells relative to T eff cells. To distinguish these alternatives, we used *B6.Foxp3^{gfp}* reporter mice (Fontenot et al., 2005). We performed mixed aHSCT with WT and *Foxp3^{gfp}* mice as donors, using purified GFP-negative cells from *Foxp3^{gfp}* mice to remove preexisting T reg cells from the donor population. In this mixed aHSCT setting, 6A6 treatment similarly decreased the accumulation of T eff cells in both populations, but T reg cells expanded only from preexisting T reg cells (Fig. 2, f and g; and Fig. S2, e and f). Therefore, the donor T reg/T eff cell ratio increased only among the WT donor T cells and not in the *Foxp3^{gfp}* donor T cells, as assessed by intracellular staining for endogenous Foxp3 (Fig. 2 f and Fig. S2 g). In addition, donor-derived CD4+ T cells, which were originally isolated from *B6.Foxp3^{gfp}* mice as negative for GFP expression, remained negative for Foxp3 as assessed by the Foxp3-GFP reporter (Fig. S2 e, right).

To further characterize the conditions necessary for the expansion of T reg cells, we evaluated what effects anti-BTLA treatment had on T reg cells in the steady state and whether the presence of alloantigen or HVEM on host tissue is required. When unmanipulated *B6.Foxp3^{gfp}* mice received 6A6, the frequency of T eff cells, T reg cells, or the resulting ratio did not change (Fig. S3, a–d). Similarly, although syngeneic aHSCT of CB6F1 resulted in a small decrease of T eff cells 7 d after transplant, no major accumulation of T reg cells and no increased T reg/T eff cell ratio was observed (Fig. S3, e–h). When HVEM$^{-/-}$ donors and MHC-mismatched HVEM$^{-/-}$ recipients were used, the ratio of T reg/T eff cells increased by inhibiting the accumulation of T eff cells

Published November 15, 2010

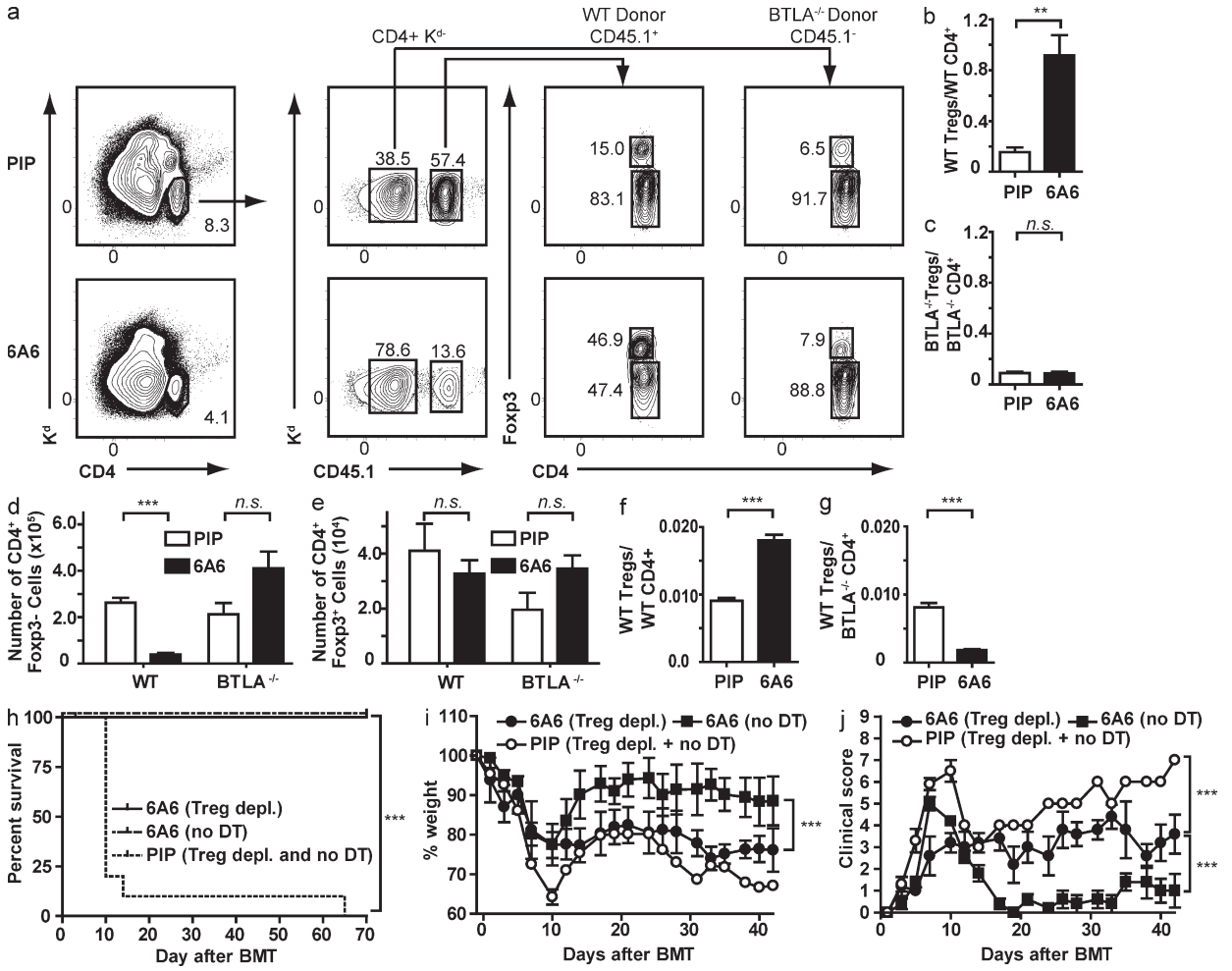

Figure 3. Direct engagement of BTLA on T eff cells leads to an increased frequency of CD4+Foxp3+ cells. Lethally irradiated CB6F1 mice received a 1:1 mixed aHSCT with WT-B6.SJL and B6 BTLA$^{-/-}$ donor cells (a–e) with either control antibody (PIP) or 6A6 (n = 5 per group). After 7 d, splenocytes were analyzed by flow cytometry. (a) Shown are FACS plots to identify donor cells as H-2K^{d-} and CD4+ (left). Intracellular Foxp3 was detected among CD4+ T cells (right) gated on WT-B6.SJL (CD4+CD45.1+ H-2K^{d-}) or B6 BTLA$^{+/+}$ (CD4+CD45.1− H-2K^{d-}) donor cell populations as indicated. Numbers represent the percentage of cells within the indicated gates. The ratios of the number of WT T reg/WT T eff cells (b) and KO T reg/ KO T eff cells (c) are shown, as well as the total number of T eff cells (d) and T reg cells (e) from the indicated donors after treatment with control antibody (PIP, open bars) or 6A6 (closed bars). (f and g) Lethally irradiated BALB/c mice received a 1:1 mixture of purified WT-B6.SJL and BTLA$^{-/-}$ CD4+ cells and T reg cells from *B6.Foxp3^{gfp}* mice, with either control antibody PIP or 6A6 (n = 3–4 per group). After 7 d, splenocytes were analyzed by flow cytometry to determine the ratio of WT T reg/WT T eff cells (f) or WT T reg/BTLA$^{-/-}$ T eff cells (g). Data are displayed as mean ± SEM. Shown are representative data from two independent experiments. (h–j) Recipient BALB/c mice received TCD-BM and splenocytes from T reg cell ablated or unmanipulated Foxp3^{DTR} mice and PIP or 6A6 as indicated. Survival curves (h), weight curves (i), and clinical scores (j) are shown for 6A6-treated mice that received a graft from either untreated (no DT) Foxp3^{DTR} donors (dashed line or filled squares; n = 5) or a graft from DT-treated (T reg depl.) Foxp3^{DTR} donors (solid line or filled circles; n = 5) and PIP-treated mice that received a graft from DT-treated or untreated (T reg depl. and no DT) Foxp3^{DTR} donors (dotted line or open circles; n = 10). Data are shown as mean ± SD from two independent experiments. P-values of >0.05 are considered not significant (n.s). **, 0.001 < P < 0.01; ***, P < 0.001.

(Fig. S3, i–l) as observed before (Fig. 2, d and g). Collectively, these results suggest that 6A6 has no effect in the steady state, does not involve HVEM, and requires allostimulation to increase the T reg/T eff cell ratio.

Because BTLA is expressed on both T eff and T reg cells, we tested whether the increased T reg/T eff cell ratio was the result of a decrease in T eff cell expansion, an increased proliferation of T reg cells, or both by performing a mixed aHSCT using congenically marked WT BTLA$^{+/+}$ and BTLA$^{-/-}$ donors. In this setting, the frequency of T reg cell within the CD4+BTLA$^{-/-}$ population did not change in the presence of 6A6 (7.9 ± 2 vs. 7.3 ± 2%; Fig. 3, a and c), whereas the T reg cell frequency within the CD4+ WT population increased more than threefold in the presence of 6A6 (48 ± 10 vs. 14.4 ± 5.5%; Fig. 3, a and b).

Importantly, 6A6 treatment decreased T eff cell numbers more than fivefold from $2.6 \times 10^5 \pm 4.6 \times 10^4$ cells in the control group to $3.9 \times 10^4 \pm 1.4 \times 10^4$ (P < 0.0001; Fig. 3 d), indicating that WT-BTLA$^{+/+}$ T eff cells are the main target of the anti-BTLA treatment. WT and BTLA$^{-/-}$ T reg cells

Published November 15, 2010

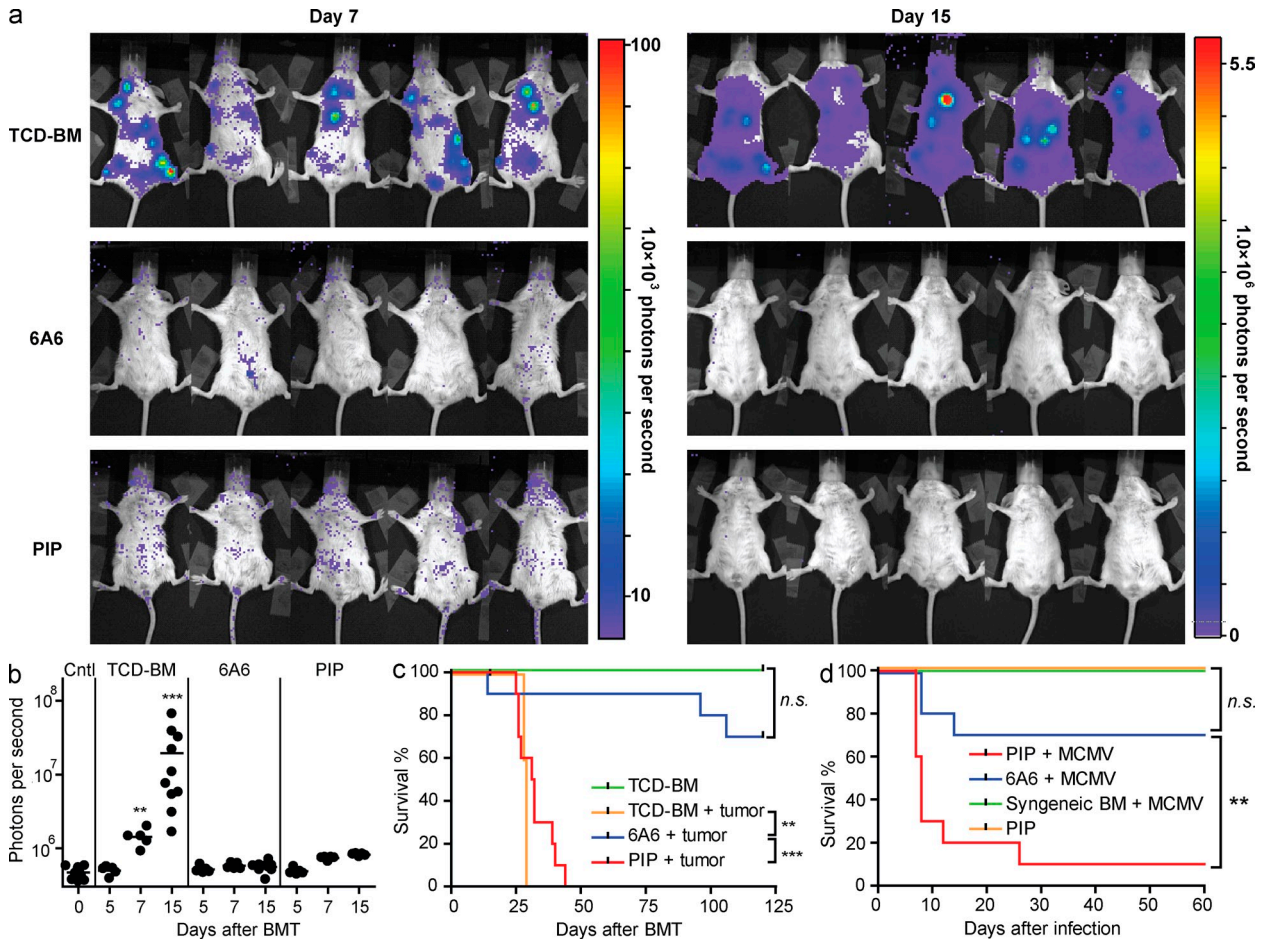

Figure 4. Anti-BTLA treatment does not lead to global immunosuppression. (a) Representative images of A20-Luc tumor cell localization 7 d (left) and 15 d (right) after aHSCT in lethally irradiated BALB/c mice that had received A20-Luc lymphoma cells with TCD-BM alone (n = 10) or together with splenocytes from C57BL/6 mice and control antibody PIP (n = 10) or 6A6 (n = 10). (b) Shown are units of photons per second for individual animals from panel a for days 5 (n = 5), 7 (n = 5), and 15 (n = 10) after aHSCT, as well as unmanipulated BALB/c mice (day 0, n = 12) for comparison. Asterisks indicate statistically significant differences between TCD-BM and 6A6 groups. Shown are cumulative data from two independent experiments, with each point representing the BLI signal from an individual mouse. Horizontal lines represent the mean BLI signal. Vertical lines serve to separate experimental groups. (c) Survival data of mice from a and from mice that received TCD-BM alone without tumor for comparison. Shown are cumulative data from two independent experiments. (d) CB6F1 BMC and splenocytes from syngeneic (green line; n = 10) or C57BL/6 donors and antibodies PIP (red line; n = 10) or 6A6 (blue line; n = 10) were infected with MCMV 4 wk after aHSCT and were monitored for survival. PIP-treated uninfected mice (orange line, n = 10) served as controls. Shown are cumulative data from two independent experiments. Data are shown as mean ± SD from two independent experiments. P-values of >0.05 are considered not significant (n.s). **, 0.001 < P < 0.01; ***, P < 0.001.

do not expand significantly in the presence of BTLA$^{-/-}$ T eff cells (Fig. 3 e), confirming our observation that T reg cells expand only when T eff cells express BTLA and are inhibited by 6A6. To exclude any indirect effects on host tissues, we cotransferred purified populations of WT T reg cells together with WT or BTLA$^{-/-}$ T eff cells into BALB/c recipients, which express an allele of BTLA not recognized by 6A6 (Fig. 3, f and g; and Fig. S4; Hurchla et al., 2005). The WT T reg/WT T eff cell ratio increased after 6A6 treatement (P < 0.0004; Fig. 3 f) as observed before (Fig. 2 g and Fig. 3 b). In contrast, when BTLA$^{-/-}$ T eff cells were present the WT T reg/BTLA$^{-/-}$ T eff cell ratio did not increase (Fig. 3 g), indicating that the expansion of T reg cells is caused by 6A6 reducing the expansion of T eff cells. In this setting, the WT T reg/BTLA$^{-/-}$ T eff cell ratio even decreased (Fig. 3 g and Fig. S4 i), suggesting that low expression levels of BTLA on T reg cells inhibits their expansion when proliferation of BTLA$^{-/-}$ T eff cells is not restricted.

To ask whether the inhibition of T eff cells had an effect on GVHD in the absence of T reg cells, we used C57BL/6 Foxp3^{DTR} mice as donors in the lethal model of GVHD. Pretreatment with diphtheria toxin reduced T reg cells by >95% in Foxp3^{DTR} donors. 90% of control animals died within 14 d of aHSCT, irrespective of whether or not the BM graft contained T reg cells (Fig. 3 h). All mice that were treated with the 6A6 antibody survived beyond day 70 (Fig. 3 h). Mice that received a graft with T reg cells and 6A6 eventually recovered to ∼90% of their starting weight (Fig. 3 i) and developed

Published November 15, 2010

low-grade GVHD with scores ranging from 1 to 3, as seen before (Fig. 1 e). Mice that received a T reg cell–depleted graft and 6A6, however, recovered only 70–80% of their starting weight and had more severe GVHD scores ranging from 3 to 5 (Fig. 3 j). These data highlight that forced inhibition of T eff cells through BTLA (Fig. 3 d) is sufficient to prevent lethality. Nonetheless, the relative expansion of T reg cells (Fig. 3, b and f) bears biological significance, as they are required to protect the host from clinical GVHD (Fig. 3, i and j).

Because engagement of BTLA by 6A6 inhibited T eff cell proliferation, we wondered whether this treatment allowed for antigen-specific responses to tumors and pathogens. First, we examined whether graft-versus-tumor (GVT) activity was maintained after 6A6 treatment (Fig. 4, a–c). We used a model of minimal residual disease after aHSCT that utilizes bioluminescence imaging (BLI) of luciferase-expressing A20-Luc leukemia cells (H-2^d) in vivo (Edinger et al., 2003a). In this model, GVT activity requires cytolytic activity of T cells to control the tumor (Edinger et al., 2003b). Transplantation of A20-Luc leukemia cells with TCD-BM alone resulted in progressive tumor growth (Fig. 4, a and b). In mice that had received a T cell–containing graft with or without the 6A6 antibody, however, tumor was never detectable by BLI, suggesting that GVT effects were intact. Although all control mice died before day 45 of severe GVHD, 90% of 6A6-treated mice survived beyond day 90 (Fig. 4 c). To exclude any antibody-mediated antitumor effects, we confirmed that the 6A6 antibody does not bind to A20 cells, which was expected because of their BALB/c origin (Fig. S2 d). To document initial tumor engraftment, we quantified the total tumor number A20-GFP cells in the BM by flow cytometry 7 d after aHSCT (Fig. S3 m).

We next examined immune responses to murine CMV (MCMV; Nguyen et al., 2008) 4 wk after aHSCT. All animals that had undergone syngeneic aHSCT survived for >60 d after infection (Fig. 4 d). Of the mice in the allogeneic group that had received the PIP antibody, 70% died within 10 d of infection compared with 20% of the 6A6-treated mice. Thus, although 6A6 treatment prevents GVHD, it allows for resistance to MCMV, unlike PIP-treated control recipients.

To test the immune response against bacterial infection, animals were infected with the intracellular bacterium *Listeria monocytogenes*. 3 d after infection, animals that had received the PIP antibody had either higher ($P = 0.0005$ for liver and $P = 0.1816$ for spleen) or lower *L. monocytogenes* organ burdens ($P = 0.0227$ for liver and $P = 0.0059$ for spleen; Fig. S3, n–p), as has been described previously (Miura et al., 2000). In contrast, anti-BTLA–treated mice controlled infection similarly to both control groups, indicating an intact innate immune response (Fig. S3, n–p). These preliminary results suggest that 6A6-treated mice were similarly resistant to *L. monocytogenes* infection to unmanipulated mice.

In summary, this study demonstrates that the anti-BTLA antibody 6A6 administered at the time of aHSCT prevents GVHD without the need for additional immunosuppressive therapy. The mechanism of action is through direct engagement of BTLA on donor T cells, selectively inhibiting T eff cells and allowing the relative expansion of naturally occurring T reg cells. Once established, this new balance of T eff cells is sufficient to prevent GVHD permanently while allowing for intact responses to viral and bacterial pathogens, as well as GVT effects. Thus, BTLA may represent a novel therapeutic target in prevention of human GVHD. Increasing the safety of aHSCT could potentially allow its application more widely as a tolerogenic therapy in treatment of autoimmune disorders or solid organ transplantation, for which it is currently performed only experimentally (Sykes and Nikolic, 2005; Kawai et al., 2008).

MATERIALS AND METHODS

Mice and BM transplantation. B6.SJL-Ptprca Pep3b/BoyJ (B6.SJL), C57BL/6, and C57BL/6 × BALB/c F1 (CB6F1) mice were obtained from The Jackson Laboratory or bred in our facility. *BTLA*$^{-/-}$ (Watanabe et al., 2003), *Hvem*$^{-/-}$ (Wang et al., 2005), *Foxp3*^{gfp} (Fontenot et al., 2005), and *Foxp3*^{DTR} (Kim et al., 2007) mice were backcrossed to C57BL/6 for at least nine generations. HVEM$^{-/-}$ H2-K$^{b/d}$ or H2-K$^{d/d}$ were obtained by crossing HVEM$^{-/-}$ mice on a B6 (H2-K$^{b/b}$) background to BALB/c (H2-K$^{d/d}$) mice. The resulting HVEM$^{+/-}$ H2-K$^{d/b}$ F1 mice were intercrossed to obtain HVEM$^{-/-}$ H2-K$^{b/d}$ or H2-K$^{d/d}$ F2 recipients. Mice were 12–18 wk old and sex matched for all experiments. Mice were bred and maintained in our specific pathogen–free animal facility according to institutional guidelines with protocols approved by the Animal Studies Committee of Washington University.

Cell transplantation and assessment of GVHD. Mice received transplants according to a standard protocol as previously described (Stelljes et al., 2008). In brief, BMCs were harvested by flushing tibia and femurs of donor mice. For the nonlethal parent-into-F1 model of GVHD, CB6F1 (H-$2^{b/d}$) recipients were lethally irradiated with 9 Gy total body irradiation using a ^{137}Cs source at a dose rate of ∼70 cGy/min and reconstituted with 2×10^7 BMCs and 10^7 splenocytes from syngeneic (H-$2^{b/d}$) or parental C57BL/6 donors (H-2^b). For the lethal model of GVHD, BALB/c (H-2^d) recipients were lethally irradiated with 8 Gy total body irradiation using a ^{137}Cs source at a dose rate of ∼70 cGy/min and reconstituted with 2×10^7 TCD-BM alone or an additional 10^7 splenocytes from allogeneic C57BL/6 donors (H-2^b). To obtain TCD-BM, cells were depleted of CD4$^+$ and CD8$^+$ cells by magnetic depletion (Miltenyi Biotec) according to the manufacturer's recommendation. In experiments where a T reg cell–depleted graft from *Foxp3*^{DTR} donors was used, recipients received an intraperitoneal injection of 20 μg diphtheria toxin on the day of BMT. GVHD was monitored by calculating the loss in total body weight. Body weights were measured before transplantation and three times a week after transplantation. Clinical GVHD intensity was scored by assessing weight loss, posture, activity, fur texture, and skin integrity (Cooke et al., 1996). Histopathologic analyses of the bowel were performed on hematoxylin and eosin–stained tissue.

Administration of antibody. In some experiments, mice received at the time of aHSCT, unless otherwise noted, a single intraperitoneal injection of 10–20 μg/g body weight of anti-BTLA antibodies 6A6 and 6F7, whose properties we have previously published in detail (Hurchla et al., 2005). In brief, the IgG hamster monoclonal antibody 6A6 is specific for the C57BL/6 allele of BTLA and does not deplete BTLA-expressing cells in vivo (Hurchla et al., 2007; Lepenies et al., 2007). The IgG1κ mouse monoclonal anti-BTLA antibody 6F7 recognizes all known alleles of BTLA (Hurchla et al., 2005) and has been shown to deplete BTLA-expressing cells in vivo. The IgG1 hamster monoclonal anti-GST antibody PIP (Gronowski et al., 1999) was used as an isotype control.

Cell purification and depletion. To obtain purified populations of CD4$^+$ Foxp3^{gfp}-negative cells or CD4$^+$ Foxp3^{gfp}-positive cells in the indicated experiments, Foxp3^{gfp} splenocytes were stained with CD4$^+$ and the desired population was purified by cell sorting on the MoFlo cytometer (Dako).

Published November 15, 2010

Purification of C57BL/6 $CD4^+$ and $BTLA^{-/-}$ $CD4^+$ cells was obtained from splenocytes that were depleted of $CD8^+$ and $B220^+$ cells by magnetic depletion (Miltenyi Biotech) according to the manufacturer's recommendation. *Foxp3*^{DTR} mice received intraperitoneal injections for 2 d of 20 µg diphtheria toxin per day before harvesting BM and splenocytes for aHSCT.

CFSE labeling and flow cytometry. Cells were labeled with CFSE (Sigma-Aldrich) by being incubated for 8 min at 25°C with 1 µM CFSE at a density of 40×10^6 cells per ml in PBS. Labeling was quenched by incubation of cells for 1 min with an equal volume of FCS and cells were washed twice with media containing 10% (vol/vol) FCS. 50×10^6 total cells per mouse were injected intravenously. Single cell suspensions from spleens were analyzed by flow cytometry using the following antibodies for detection: K^d-FITC (SF1-1.1), CD4-PECy7, APC, PerCPCy5.5, v450 (RM4-5) and PE (GK1.5), CD8-v450 (53–6.7), anti–Armenian and Syrian hamster IgG cocktail-PE, CD19-APC (1D3), and annexin V–PE (BD); and CD45.1-PECy7 and APC (A20), CD45.2-APC-eFluor780 (104), CD8-APC Alexa Fluor 750 (53–6.7), CD4-APC Alexa Fluor 750 (RM4-5), BTLA-bio (6F7), and SA-v450 (eBioscience). Intracellular Foxp3 was detected using the Mouse Regulatory T cell staining kit (eBioscience) with Foxp3-PE or APC (FJK-16s). For intracellular cytokine staining, splenocytes were first restimulated with PMA/ionomycin for 4 h and were stained with antibodies to surface markers, followed by fixation with 2% formaldehyde for 15 min at room temperature. Cells were then washed once in 0.05% saponin and stained with anti-cytokine antibodies (anti-IL-17 FITC, IL-2 PE, IFN-γ PE-Cy7, and IL-4 APC) in 0.5% saponin. All flow cytometry data were collected on a FACSCanto II (BD) and were analyzed with FlowJo software (Tree Star, Inc.).

Tumor model and assessment of GVT effects. As a tumor challenge, 2×10^4 A20-Luc or A20-GFP where administered intravenously together with the donor graft as indicated. Imaging was done as previously described (Rehemtulla et al., 2000; Edinger et al., 2003a). In brief, D-Luciferin (Biosynth AG) was reconstituted in 0.9% sodium chloride (Baxter) to a concentration of 15 mg/ml, filtered (0.2 µm), and frozen at −80°C until use. Mice were given intraperitoneal injections at a dose of 150 mg/kg and allowed to remain active in the cage for 5 min to allow circulation of luciferin. Using the Xenogen IVIS 200 system (Caliper Life Sciences) with attached anesthesia chamber, the animals were then anesthetized with 2% isoflurane for 5 min and subsequently transferred to the imaging chamber where they continued to receive a regulated flow of isoflurane through the manifold's nose cones. The Living Image software program (Caliper Life Sciences) was used to obtain and analyze data. For all experiments, a 60-s exposure time was used. To detect A20-GFP in the BM, single cell suspensions from both femurs were analyzed by flow cytometry using the antibody CD19-APC (1D3; BD). Cells that expressed high levels of CD19 and GFP were considered to be A20-GFP cells.

Cell lines. The BALB/c B cell lymphoma cell line A20 was obtained from the American Type Culture Collection. To generate luciferase-expressing A20 cells (A20-Luc), a 1995-bp HindIII–BamHI fragment from pGL4.23[luc2/minP] vector (Promega) containing a minimal promoter, a Luc2 coding sequence, and a SV40 late poly(A) signal was cloned into the HindIII and BamHI sites of the pcDNA3.1$^+$ mammalian expression vector (Invitrogen) to generate pcDNA3.1$^+$-Luc2. For stable transfections, 10×10^6 A20 cells/ml in complete IMDM supplemented with 10% fetal calf serum and with 30 µg/ml PvuI-linearized pcDNA3.1$^+$-Luc2 were electroporated at room temperature in 0.4-ml aliquots in 0.4-cm cuvettes in a Gene Pulser (Bio-Rad Laboratories) at 240 V and 960 mF. After electroporation, cells were cultured for 24 h in IMDM supplemented with 10% fetal calf serum and then selected in the presence of 800 µg/ml geneticin. To generate GFP-expressing A20 cells, a retroviral reporter vector (Ranganath et al., 1998) was used that contains the coding sequence of herpes simplex virus 1 thymidine kinase, followed by an internal ribosomal entry site and GFP (HSV1-TK-IRES-GFP-RV). The retroviral vector was packaged in Phoenix A cells. Before infection, the A20 cell line was stimulated with 5 µg/ml LPS (Sigma-Aldrich) for 24 h. For infection, cells were cultured in retroviral supernatant supplemented with 8 µg/ml polybrene (Sigma-Aldrich) and 5 µg/ml LPS and spun at 930 rcf for 1 h before being cultured at 37°C for 24 h. 72 h after infection, cells were sorted for high GFP expression on a FACSAria II (BD) and stable GFP expression of >95% was confirmed several times by flow cytometry at later time points.

Models of infectious disease. For MCMV infection, mice were infected with Smith strain MCMV 4 wk after aHSCT. Virus preparation and administration was performed as described previously (Krug et al., 2004). In brief, a salivary gland stock of MCMV was prepared from BALB/c mice, with a titer of 6.75×10^6 PFU/ml. Mice were infected intraperitoneally with a low dose of virus (10^4 PFU/mouse) and then monitored for survival. For *L. monocytogenes* infection, mice were infected intravenously with 2.5×10^4 *L. monocytogenes* (strain EGD; gift from E.R. Unanue, Washington University School of Medicine, St. Louis, MO) 3 mo after aHSCT. To determine organ *L. monocytogenes* burden at day 3 after infection, spleens and livers were homogenized in PBS plus 0.05% Triton X-100. Serial dilutions of homogenate were plated on brain heart infusion agar, and bacterial CFUs were assessed after overnight growth at 37°C. Small portions of spleen and liver were also fixed in 10% formalin and stained with hematoxylin and eosin.

Statistical analysis. A Student's unpaired two-tailed *t* test with a 95% confidence interval was used for statistical analyses of body weight data, clinical scores, and cell numbers. For analyses of survival data the log-rank test was used. A Mann-Whitney unpaired two-tailed Student's *t* test with a 95% confidence interval was used for statistical analyses of bioluminescence data in Fig. 4. Statistical analyses were done using Prism 4 (GraphPad Software, Inc.). FACS data are expressed as means ± SEM. All other data are presented as means ± SD. All experiments have been repeated at least once with three to five mice per group, unless stated otherwise.

Online supplemental material. Fig. S1 demonstrates that BTLA expression by recipient tissue does not promote GVHD and 6A6 antibody does not deplete lymphocytes. Fig. S2 shows that 6A6 treatment does not lead to donor T eff cell anergy and expands preexisting T reg cells. Fig. S3 shows that 6A6 inhibition of T eff cells and expansion of T reg cells requires allostimulation but not HVEM expression by donor or host. Fig. S4 shows that 6A6 alters the T reg cell/effector $CD4^+$ T cell ratio by directly inhibiting BTLA-expressing T cells. Online supplemental material is available at http://www.jem.org/cgi/content/full/jem.20102017/DC1.

The authors thank T.S. Stappenbeck for help with histology and T.R. Bradstreet for help with *L. monocytogenes* experiments.

K.M. Murphy is a Howard Hughes Medical Institute investigator. This work was supported in part by the National Institutes of Health (AI076427-02) and the Department of Defense (W81XWH-09-1-0185). J.C. Albring was supported by a German Research Foundation Grant (AL 1038/1-1). M.M. Sandau was supported by a Ruth L. Kirschstein National Reasearch Service Award (NIH # 5F32AI080062-02) and by the Irvington Institute Fellowship Program of the Cancer Research Institute. B.T. Edelson was supported by the Burroughs Wellcome Fund Career Award for Medical Scientists.

The authors have no conflicting financial interests.

Submitted: 24 September 2010
Accepted: 29 October 2010

REFERENCES

Blazar, B.R., B.M. Carreno, A. Panoskaltsis-Mortari, L. Carter, Y. Iwai, H. Yagita, H. Nishimura, and P.A. Taylor. 2003. Blockade of programmed death-1 engagement accelerates graft-versus-host disease lethality by an IFN-gamma-dependent mechanism. *J. Immunol.* 171:1272–1277.

Chen, W., W. Jin, N. Hardegen, K.J. Lei, L. Li, N. Marinos, G. McGrady, and S.M. Wahl. 2003. Conversion of peripheral $CD4^+CD25^-$ naive T cells to $CD4^+CD25^+$ regulatory T cells by TGF-β induction of transcription factor Foxp3. *J. Exp. Med.* 198:1875–1886. doi:10.1084/jem.20030152

Cooke, K.R., L. Kobzik, T.R. Martin, J. Brewer, J. Delmonte Jr., J.M. Crawford, and J.L.M. Ferrara. 1996. An experimental model of idiopathic pneumonia syndrome after bone marrow transplantation: I. The roles of minor H antigens and endotoxin. *Blood.* 88:3230–3239.

Copelan, E.A. 2006. Hematopoietic stem-cell transplantation. *N. Engl. J. Med.* 354:1813–1826. doi:10.1056/NEJMra052638

Edinger, M., Y.A. Cao, M.R. Verneris, M.H. Bachmann, C.H. Contag, and R.S. Negrin. 2003a. Revealing lymphoma growth and the efficacy of immune cell therapies using in vivo bioluminescence imaging. *Blood.* 101:640–648. doi:10.1182/blood-2002-06-1751

Edinger, M., P. Hoffmann, J. Ermann, K. Drago, C.G. Fathman, S. Strober, and R.S. Negrin. 2003b. CD4+CD25+ regulatory T cells preserve graft-versus-tumor activity while inhibiting graft-versus-host disease after bone marrow transplantation. *Nat. Med.* 9:1144–1150. doi:10.1038/nm915

Fontenot, J.D., J.P. Rasmussen, L.M. Williams, J.L. Dooley, A.G. Farr, and A.Y. Rudensky. 2005. Regulatory T cell lineage specification by the forkhead transcription factor foxp3. *Immunity.* 22:329–341. doi:10.1016/j.immuni.2005.01.016

Gavrieli, M., and K.M. Murphy. 2006. Association of Grb-2 and PI3K p85 with phosphotyrosile peptides derived from BTLA. *Biochem. Biophys. Res. Commun.* 345:1440–1445. doi:10.1016/j.bbrc.2006.05.036

Gronowski, A.M., D.M. Hilbert, K.C.F. Sheehan, G. Garotta, and R.D. Schreiber. 1999. Baculovirus stimulates antiviral effects in mammalian cells. *J. Virol.* 73:9944–9951.

Hori, S., T. Nomura, and S. Sakaguchi. 2003. Control of regulatory T cell development by the transcription factor Foxp3. *Science.* 299:1057–1061. doi:10.1126/science.1079490

Hurchla, M.A., J.R. Sedy, M. Gavrieli, M. Gavrielli, C.G. Drake, T.L. Murphy, and K.M. Murphy. 2005. B and T lymphocyte attenuator exhibits structural and expression polymorphisms and is highly induced in anergic CD4+ T cells. *J. Immunol.* 174:3377–3385.

Hurchla, M.A., J.R. Sedy, and K.M. Murphy. 2007. Unexpected role of B and T lymphocyte attenuator in sustaining cell survival during chronic allostimulation. *J. Immunol.* 178:6073–6082.

Kawai, T., A.B. Cosimi, T.R. Spitzer, N. Tolkoff-Rubin, M. Suthanthiran, S.L. Saidman, J. Shaffer, F.I. Preffer, R.C. Ding, V. Sharma, et al. 2008. HLA-mismatched renal transplantation without maintenance immunosuppression. *N. Engl. J. Med.* 358:353–361. doi:10.1056/NEJMoa071074

Kim, J.M., J.P. Rasmussen, and A.Y. Rudensky. 2007. Regulatory T cells prevent catastrophic autoimmunity throughout the lifespan of mice. *Nat. Immunol.* 8:191–197. doi:10.1038/ni1428

Krug, A., A.R. French, W. Barchet, J.A.A. Fischer, A. Dzionek, J.T. Pingel, M.M. Orihuela, S. Akira, W.M. Yokoyama, and M. Colonna. 2004. TLR9-dependent recognition of MCMV by IPC and DC generates coordinated cytokine responses that activate antiviral NK cell function. *Immunity.* 21:107–119. doi:10.1016/j.immuni.2004.06.007

Lepenies, B., K. Pfeffer, M.A. Hurchla, T.L. Murphy, K.M. Murphy, J. Oetzel, B. Fleischer, and T. Jacobs. 2007. Ligation of B and T lymphocyte attenuator prevents the genesis of experimental cerebral malaria. *J. Immunol.* 179:4093–4100.

Liu, X.K., M. Alexiou, N. Martin-Orozco, Y. Chung, R.I. Nurieva, L. Ma, Q. Tian, G. Kollias, S. Lu, D. Graf, and C. Dong. 2009. Cutting edge: A critical role of B and T lymphocyte attenuator in peripheral T cell tolerance induction. *J. Immunol.* 182:4516–4520. doi:10.4049/jimmunol.0803161

Lu, Y., S. Sakamaki, H. Kuroda, T. Kusakabe, Y. Konuma, T. Akiyama, A. Fujimi, N. Takemoto, K. Nishiie, T. Matsunaga, et al. 2001. Prevention of lethal acute graft-versus-host disease in mice by oral administration of T helper 1 inhibitor, TAK-603. *Blood.* 97:1123–1130. doi:10.1182/blood.V97.4.1123

McSweeney, P.A., D. Niederwieser, J.A. Shizuru, B.M. Sandmaier, A.J. Molina, D.G. Maloney, T.R. Chauncey, T.A. Gooley, U. Hegenbart, R.A. Nash, et al. 2001. Hematopoietic cell transplantation in older patients with hematologic malignancies: replacing high-dose cytotoxic therapy with graft-versus-tumor effects. *Blood.* 97:3390–3400. doi:10.1182/blood.V97.11.3390

Miura, T., D. Mizuki, S. Sasaki, S. Hasegawa, H. Sashinami, and A. Nakane. 2000. Host resistance to *Listeria monocytogenes* infection is enhanced but resistance to *Staphylococcus aureus* infection is reduced in acute graft-versus-host disease in mice. *Infect. Immun.* 68:4340–4343. doi:10.1128/IAI.68.7.4340-4343.2000

Nguyen, V.H., S. Shashidhar, D.S. Chang, L. Ho, N. Kambham, M. Bachmann, J.M. Brown, and R.S. Negrin. 2008. The impact of regulatory T cells on T-cell immunity following hematopoietic cell transplantation. *Blood.* 111:945–953. doi:10.1182/blood-2007-07-103895

Petersdorf, E.W., C. Anasetti, P.J. Martin, T. Gooley, J. Radich, M. Malkki, A. Woolfrey, A. Smith, E. Mickelson, and J.A. Hansen. 2004. Limits of HLA mismatching in unrelated hematopoietic cell transplantation. *Blood.* 104:2976–2980. doi:10.1182/blood-2004-04-1674

Ranganath, S., W. Ouyang, D. Bhattarcharya, W.C. Sha, A. Grupe, G. Peltz, and K.M. Murphy. 1998. GATA-3-dependent enhancer activity in IL-4 gene regulation. *J. Immunol.* 161:3822–3826.

Rehemtulla, A., L.D. Stegman, S.J. Cardozo, S. Gupta, D.E. Hall, C.H. Contag, and B.D. Ross. 2000. Rapid and quantitative assessment of cancer treatment response using in vivo bioluminescence imaging. *Neoplasia.* 2:491–495. doi:10.1038/sj.neo.7900121

Sedy, J.R., M. Gavrieli, K.G. Potter, M.A. Hurchla, R.C. Lindsley, K. Hildner, S. Scheu, K. Pfeffer, C.F. Ware, T.L. Murphy, and K.M. Murphy. 2005. B and T lymphocyte attenuator regulates T cell activation through interaction with herpesvirus entry mediator. *Nat. Immunol.* 6:90–98. doi:10.1038/ni1144

Steinberg, M.W., O. Turovskaya, R.B. Shaikh, G. Kim, D.F. McCole, K. Pfeffer, K.M. Murphy, C.F. Ware, and M. Kronenberg. 2008. A crucial role for HVEM and BTLA in preventing intestinal inflammation. *J. Exp. Med.* 205:1463–1476. doi:10.1084/jem.20071160

Stelljes, M., S. Hermann, J. Albring, G. Köhler, M. Löffler, C. Franzius, C. Poremba, V. Schlösser, S. Volkmann, C. Opitz, et al. 2008. Clinical molecular imaging in intestinal graft-versus-host disease: mapping of disease activity, prediction, and monitoring of treatment efficiency by positron emission tomography. *Blood.* 111:2909–2918. doi:10.1182/blood-2007-10-119164

Sykes, M., and B. Nikolic. 2005. Treatment of severe autoimmune disease by stem-cell transplantation. *Nature.* 435:620–627. doi:10.1038/nature03728

Tamada, K., K. Shimozaki, A.I. Chapoval, G. Zhu, G. Sica, D. Flies, T. Boone, H. Hsu, Y.X. Fu, S. Nagata, et al. 2000. Modulation of T-cell-mediated immunity in tumor and graft-versus-host disease models through the LIGHT co-stimulatory pathway. *Nat. Med.* 6:283–289. doi:10.1038/73136

Taylor, P.A., C.J. Lees, and B.R. Blazar. 2002. The infusion of ex vivo activated and expanded CD4(+)CD25(+) immune regulatory cells inhibits graft-versus-host disease lethality. *Blood.* 99:3493–3499. doi:10.1182/blood.V99.10.3493

Truong, W., W.W. Hancock, J.C. Plester, S. Merani, D.C. Rayner, G. Thangavelu, K.M. Murphy, C.C. Anderson, and A.M. Shapiro. 2009. BTLA targeting modulates lymphocyte phenotype, function, and numbers and attenuates disease in nonobese diabetic mice. *J. Leukoc. Biol.* 86:41–51. doi:10.1189/jlb.1107753

Wang, Y., S.K. Subudhi, R.A. Anders, J. Lo, Y. Sun, S. Blink, Y. Wang, J. Wang, X. Liu, K. Mink, et al. 2005. The role of herpesvirus entry mediator as a negative regulator of T cell-mediated responses. *J. Clin. Invest.* 115:711–717.

Watanabe, N., M. Gavrieli, J.R. Sedy, J. Yang, F. Fallarino, S.K. Loftin, M.A. Hurchla, N. Zimmerman, J. Sim, X. Zang, et al. 2003. BTLA is a lymphocyte inhibitory receptor with similarities to CTLA-4 and PD-1. *Nat. Immunol.* 4:670–679. doi:10.1038/ni944

Wu, T.H., Y. Zhen, C. Zeng, H.F. Yi, and Y. Zhao. 2007. B and T lymphocyte attenuator interacts with CD3zeta and inhibits tyrosine phosphorylation of TCRzeta complex during T-cell activation. *Immunol. Cell Biol.* 85:590–595. doi:10.1038/sj.icb.7100087

Xu, Y., A.S. Flies, D.B. Flies, G. Zhu, S. Anand, S.J. Flies, H. Xu, R.A. Anders, W.W. Hancock, L. Chen, and K. Tamada. 2007. Selective targeting of the LIGHT-HVEM costimulatory system for the treatment of graft-versus-host disease. *Blood.* 109:4097–4104. doi:10.1182/blood-2006-09-047332

Cross-dressed CD8α$^+$/CD103$^+$ dendritic cells prime CD8$^+$ T cells following vaccination

Lijin Li[a], Sojung Kim[b], John M. Herndon[a], Peter Goedegebuure[a,c], Brian A. Belt[a], Ansuman T. Satpathy[b], Timothy P. Fleming[a,c], Ted H. Hansen[b,c], Kenneth M. Murphy[b,c,d], and William E. Gillanders[a,c,1]

Departments of [a]Surgery and [b]Pathology and Immunology and [d]The Howard Hughes Medical Institute, Washington University School of Medicine, St. Louis, MO 63110; and [c]The Alvin J. Siteman Cancer Center, Barnes–Jewish Hospital and Washington University School of Medicine, St. Louis, MO 63110

Edited by Michael J. Bevan, University of Washington, Seattle, WA, and approved June 19, 2012 (received for review February 27, 2012)

Activation of naïve cluster of differentiation (CD)8$^+$ cytotoxic T lymphocytes (CTLs) is a tightly regulated process, and specific dendritic cell (DC) subsets are typically required to activate naive CTLs. Potential pathways for antigen presentation leading to CD8$^+$ T-cell priming include direct presentation, cross-presentation, and cross-dressing. To distinguish between these pathways, we designed single-chain trimer (SCT) peptide–MHC class I complexes that can be recognized as intact molecules but cannot deliver antigen to MHC through conventional antigen processing. We demonstrate that cross-dressing is a robust pathway of antigen presentation following vaccination, capable of efficiently activating both naïve and memory CD8$^+$ T cells and requires CD8α$^+$/CD103$^+$ DCs. Significantly, immune responses induced exclusively by cross-dressing were as strong as those induced exclusively through cross-presentation. Thus, cross-dressing is an important pathway of antigen presentation, with important implications for the study of CD8$^+$ T-cell responses to viral infection, tumors, and vaccines.

Professional antigen-presenting cells (APCs) are typically required to activate naïve cluster of differentiation (CD)8$^+$ T cells, either by direct priming or cross-priming. In direct priming, infected (viral infection) or directly transfected (DNA vaccination) APCs synthesize the foreign antigen and use endogenous MHC class I pathways of antigen presentation to present antigen and prime CD8$^+$ T cells. In cross-priming, APCs are able to capture, process, and present exogenous antigen onto MHC class I molecules through a process known as cross-presentation (1). Cross-priming has been shown to be an essential pathway for immunity to many viral infections and tumors. Although the pathways that lead to cross-presentation remain incompletely understood, increasing evidence suggests that only certain dendritic cell (DC) subsets are efficient in this process.

Cross-dressing involves the transfer of intact MHC class I/peptide complexes between cells without the requirement for further processing, representing an alternative pathway of indirect antigen presentation (2, 3). Although cross-dressed DCs can activate memory CD8$^+$ T cells following viral infection in vivo (4), it remains unclear whether cross-dressing can prime naïve CD8$^+$ T-cell responses, what DC subtypes are required to prime CD8$^+$ T cells by cross-dressing, and how robust this pathway is compared with traditional pathways of indirect antigen presentation. These questions must be addressed before the physiologic relevance of cross-dressing can be evaluated in context.

To address these questions, we have taken advantage of *Batf3*-deficient mice and engineered MHC class I single chain trimer (SCT) constructs. *Batf3*$^{-/-}$ mice have a selective loss of CD8α$^+$ and CD103$^+$ DCs, without abnormalities in other hematopoietic cell types or architecture (5). DCs from *Batf3*$^{-/-}$ mice are deficient in cross-presentation, and cytotoxic T lymphocyte (CTL) responses to viral infection and syngeneic tumors are impaired in *Batf3*$^{-/-}$ mice. Thus, *Batf3*$^{-/-}$ mice represent a valuable model system to study cross-presentation, cross-dressing, and the role of CD8α$^+$/CD103$^+$ DCs following DNA or cellular vaccination. We have previously engineered completely assembled MHC class I SCT whereby all three components of the complex (heavy chain, β_2m, and peptide) are attached by flexible linkers (6). Through progressive molecular engineering, even peptides with low binding affinities can be successfully anchored in the peptide binding groove by a disulfide trap between the first linker and the heavy chain (7–9). Using these experimental tools, we demonstrate that cross-dressing is a robust pathway of antigen presentation following DNA and cellular vaccination, capable of priming naïve and memory CD8$^+$ T cells. In addition, we demonstrate that CD8α$^+$/CD103$^+$ DCs are required to prime CTLs by cross-dressing.

Results

CD8α$^+$/CD103$^+$ DCs Are Required to Prime CD8$^+$ T Cells Following DNA Vaccination. Recently, we identified *Batf3* as a key transcription factor controlling the development of CD8α$^+$ and CD103$^+$ DCs (5). *Batf3*$^{-/-}$ mice lack CD8α$^+$/CD103$^+$ DC subsets and have reduced CD8$^+$ T-cell responses to viral infection and syngeneic tumors, but their responses to cell-based or DNA vaccines and capacity for cross-dressing have not been examined. We first measured responses in *Batf3*$^{-/-}$ mice to a DNA vaccine expressing soluble chicken ovalbumin (OVA) protein. *Batf3*$^{-/-}$ mice showed markedly reduced CD8$^+$ T-cell responses, as assessed by IFN-γ production relative to wild-type (WT) mice (Fig. 1 *A* and *B*), suggesting that conventional DNA vaccination proceeds via indirect antigen presentation. In response to immunization using the major OVA peptide epitope SIINFEKL, *Batf3*$^{-/-}$ mice showed a normal CD8$^+$ T-cell response (Fig. 1*C*), indicating that defective responses of *Batf3*$^{-/-}$ mice was not caused by an intrinsic T-cell defect. Moreover, *Batf3*$^{-/-}$ mice developed normal isotype-switched OVA-specific antibody responses (Fig. 1*D*), suggesting no significant defect in CD4$^+$ helper T-cell responses. Of note, *Batf3*$^{-/-}$ mice had normal cellular infiltrates at the immunization site (Fig. S1). Together, these results confirm a requirement for CD8α$^+$/CD103$^+$ DCs in priming CD8$^+$ T cells in response to DNA vaccination but do not determine whether these DCs obtain antigen in this setting through conventional cross-presentation or by cross-dressing.

MHC Class I SCTs Are Recognized as Intact Complexes. We previously generated SCT complexes by integrating the class I heavy chain, β_2m, and peptide with flexible linkers into a single ORF (6). SCTs are recognized by T cells in a manner equivalent to peptide–MHC complexes generated by conventional antigen processing (10–12) and induce robust immune responses when used as DNA vaccines (7, 13). Importantly, SCTs allow peptides with very weak affinity for MHC to be anchored into the peptide

Author contributions: L.L. and W.E.G. designed research; L.L., S.K., J.M.H., B.A.B., and A.T.S. performed research; T.H.H. and K.M.M. contributed new reagents/analytic tools; L.L., P.G., T.P.F., T.H.H., K.M.M., and W.E.G. analyzed data; and L.L. and W.E.G. wrote the paper.

The authors declare no conflict of interest.

This article is a PNAS Direct Submission.

[1]To whom correspondence should be addressed. E-mail: gillandersw@wustl.edu.

This article contains supporting information online at www.pnas.org/lookup/suppl/doi:10.1073/pnas.1203468109/-/DCSupplemental.

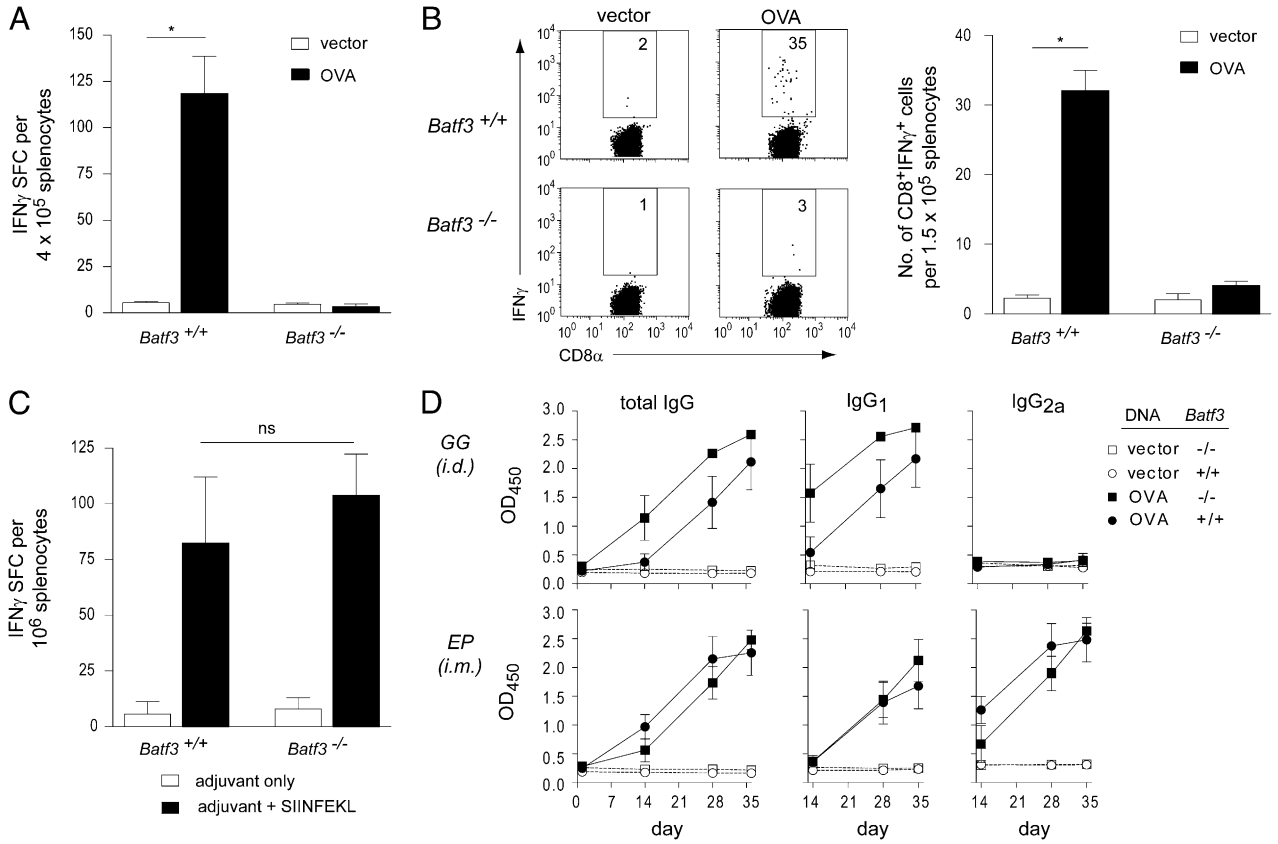

Fig. 1. CD8$^+$ T-cell priming is selectively ablated in *Batf3*$^{-/-}$ mice following DNA vaccination. (*A* and *B*) WT and *Batf3*$^{-/-}$ mice (n = 5 per group) were immunized with OVA plasmid DNA. CD8$^+$ T-cell responses were measured by IFN-γ enzyme-linked immunosorbent spot assay (ELISPOT) and intracellular cytokine staining. The results are representative of at least three independent experiments. (*C*) WT and *Batf3*$^{-/-}$ mice were vaccinated with SIINFEKL peptide and adjuvant or adjuvant alone. CD8$^+$ T-cell responses were measured by IFN-γ ELISPOT. (*D*) WT and *Batf3*$^{-/-}$ mice were vaccinated with OVA plasmid DNA. Sera were collected before and after vaccination. OVA-specific total IgG, IgG_1, and IgG_{2a} were measured by ELISA, and the levels were equivalent between WT and *Batf3*$^{-/-}$ mice. *P < 0.01; ns, not significant; SFC, spot forming cells.

binding groove through a disulfide bond between the linker and heavy chain (Fig. 2*A*) (7–9). Moreover, SCTs are recognized as intact molecules, because the D227K mutation in the α3 domain of the OVA/K^b SCT abrogates CD8 interaction (14) and induces diminished K^b-specific CD8$^+$ T-cell responses when used in a DNA vaccine (Fig. S2*A*). Similarly, a chimeric A2D^b/West Nile virus SCT showed increased responses in HHD II mice transgenic for the same chimeric A2D^b class I MHC molecules (15) (Fig. S2*B*). Together, these data show that SCT constructs are recognized as intact complexes.

p5Y SCT Cannot Be Cross-Presented by Endogenous H-2K^b. Previous studies did not exclude the possibility that the peptide in an SCT complex could additionally be cross-presented. We, therefore, generated an SCT, p5Y/K^b SCT (Fig. 2*A*), that contains an altered OVA peptide ligand SIINYEKL, which binds to K^b with a 1,000-fold lower affinity compared with the WT peptide

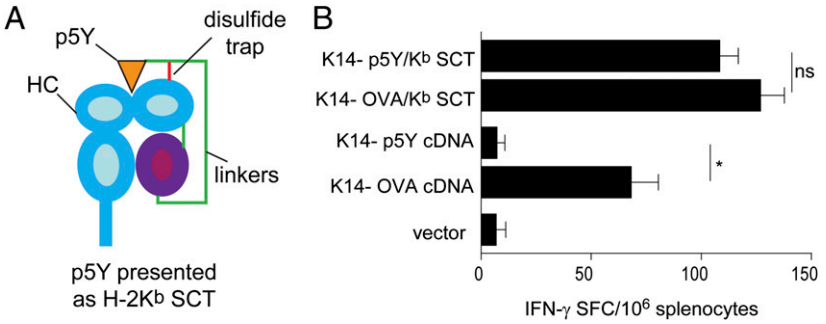

Fig. 2. Molecular engineering of SCT peptide–MHC complexes precludes cross-presentation. (*A*) Schematic of the p5Y/K^b SCT, integrating the p5Y peptide, β_2m, and H2-K^b heavy chain (HC). Of note, the disulfide bond (red line) formed between linker 1 and the α1 domain traps the low-affinity p5Y epitope in the peptide binding groove. (*B*) C57BL/6 mice (n = 4 per group) were vaccinated with the indicated DNA constructs. K^b/SIINFEKL-specific immune responses were measured by ELISPOT. Data are presented as means ± SEM. *P < 0.01; ns, not significant. Similar results were obtained in at least three independent experiments.

SIINFEKL (Fig. S3) (16). To test whether this altered peptide from the SCT could be cross-presented, we immunized mice with DNA vaccines with the keratinocyte-specific K14 promoter (17) driving expression of cDNA or SCT constructs corresponding to either WT OVA or the mutant SIINYEKL sequence (Fig. 2*B*). Immunization using WT OVA cDNA induced strong $CD8^+$ T-cell responses, but immunization with a cDNA encoding OVA with the altered SIINYEKL sequence failed to induce $CD8^+$ T-cell responses. This result indicates that the altered epitope binds too weakly to allow presentation by endogenous H-$2K^b$ MHC molecules via conventional processing pathways (16). Immunization with the SCT harboring either the WT SIINFEKL or the altered epitope SIINYEKL presented by K^b induced equally strong $CD8^+$ T-cell responses. These results show that SCTs are recognized as an intact complex and can prime T-cell responses to peptide epitopes that cannot be conventionally cross-presented because of low affinity for MHC.

Cross-Dressed DCs Prime $CD8^+$ T Cells in Vivo and in Vitro. Efficient $CD8^+$ T-cell priming after epicutaneous DNA immunization using the K14 promoter (17) suggests that SCTs are produced in keratinocytes but transferred to DCs. Alternately, T-cell priming could have resulted from direct recognition of SCTs expressed by keratinocytes and so could be independent of DCs. To test these hypotheses, we immunized WT and *Batf3*$^{-/-}$ mice with SCT DNA vaccines driven by the K14 promoter expressing the SIINYEKL epitope presented by K^b. This vaccination induced strong $CD8^+$ T-cell responses in WT mice, but $CD8^+$ T-cell responses were reduced to background in *Batf3*$^{-/-}$ mice (Fig. 3*A*). Thus, $CD8^+$ T-cell priming by vaccination with DNA encoding an SCT requires the participation of $CD8\alpha^+/CD103^+$ DCs.

Potentially, these DCs were directly transfected by the DNA vaccine to generate SCT complexes rather than obtaining these complexes from keratinocytes. To test this possibility, we stably expressed the p5Y/K^b SCT into mouse embryonic fibroblasts lacking endogenous K^b, D^b, and β2m (3KO MEFs). We adoptively transferred carboxyfluorescein diacetate succinimidyl ester (CFSE)-labeled OT-1 T cells into C57BL/6 mice, and then vaccinated mice 24 h later with necrotic 3KO p5Y/K^b SCT MEFs or 3KO MEF parental control cells. After 90 h, draining lymph nodes were harvested and OT-1 proliferation was analyzed by flow cytometry. Vaccination of WT mice with 3KO p5Y/K^b SCT MEFs, but not control parental cells, induced strong proliferation of OT-1 T cells in vivo (Fig. 3*B* and Fig. S4*A*). However, this proliferation is absent in *Batf3*$^{-/-}$ mice (Fig. 3*B*), indicating that the in vivo proliferation was not attributable to direct recognition of the p5Y/K^b SCT on MEFs but required presentation of these complexes by *Batf3*-dependent $CD8\alpha^+/CD103^+$ DCs. Vaccination with live 3KO p5Y/K^b SCT MEFs can also induce an endogenous K^b/SIINFEKL-specific immune response as measured by IFN-γ ELISPOT (Fig. S4*B*). This result suggests that the p5Y/K^b SCT expressed on MEFs was transferred to $CD8\alpha^+/CD103^+$ DCs, which induced proliferation of $CD8^+$ T cells.

To observe such transfer directly, 3KO p5Y/ K^b SCT MEFs were subjected to several freeze-thaw cycles to induce necrosis, cultured with DC2.4 DCs, and analyzed by FACS using the OVA/K^b-specific monoclonal antibody 25-D1.16 (Fig. S5*A*). A detectable increase in 25-D1.16 staining was observed on DC2.4 cells cultured with 3KO p5Y/ K^b SCT MEFs compared with DC2.4 cultured with control 3KO MEFs. Further, OT-1 T-cell proliferation was observed only when 3KO p5Y/K^b SCT MEFs and DC2.4 cells were present (Fig. S5*A*). In addition, we performed studies in vitro using the epitope-specific antibody 25.D1.16 and confocal microscopy. In these studies, we are able to demonstrate cross-dressing of intact p5Y/K^b SCT complexes from 3KO p5Y/K^b SCT MEFs to C57BL/B6 and transporter associated with antigen processing $(TAP)^{-/-}$ DCs (Fig. S5*B*). These results support the interpretation that p5Y/K^b SCT complexes are transferred from 3KO MEFs to DCs to activate OT-1 T cells.

Cross-Dressed DCs Activate both Naïve and Memory $CD8^+$ T Cells. Wakim and Bevan (4) reported that in a vesicular stomatitis virus (VSV) infection model, cross-dressed DCs activate memory, but not naïve, $CD8^+$ T cells, whereas we find that with DNA and cellular vaccines, cross-dressed DCs efficiently activate naïve $CD8^+$ T cells. To examine memory $CD8^+$ T cells, we transferred in vitro–activated OT-1 cells into C57BL/6 mice and recovered memory phenotype cells after 30 d by negative selection (Fig. S6 *A* and *B*). Memory and naïve OT-1 cells were labeled with CFSE and transferred into WT and *Batf3*$^{-/-}$ mice, which were challenged after 24 h with necrotic 3KO p5Y/ K^b SCT MEFs. Lymph nodes and spleens were harvested 90 h later, and OT-1 proliferation was examined by FACS. Vaccination with 3KO p5Y/ K^b SCT MEFs induced proliferation of both naïve and memory OT-1 cells in WT mice but not in *Batf3*$^{-/-}$ mice (Fig. S6 *C* and *D*). This result suggests that at least with cell-based immunization, cross-dressed DCs are capable of inducing proliferation in both naïve and memory $CD8^+$ T cells.

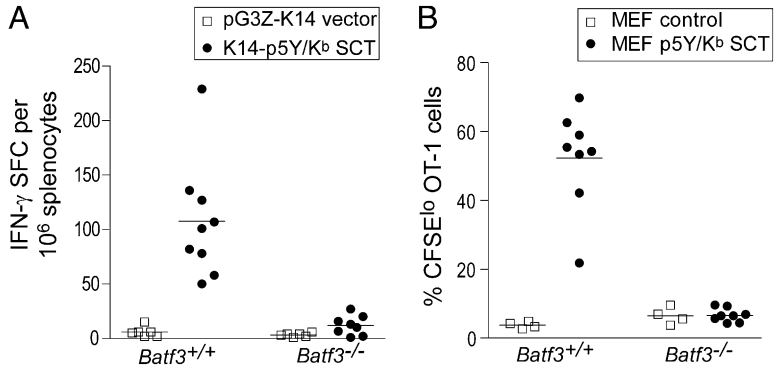

Fig. 3. Engineered SCT vaccines prime $CD8^+$ T-cell responses in vivo by cross-dressing. (*A*) WT or *Batf3*$^{-/-}$ mice were vaccinated with K14-p5Y/K^b SCT DNA or control DNA by gene gun. $CD8^+$ T-cell responses were measured by IFN-γ ELISPOT. (*B*) A total of 2×10^6 CFSE-labeled OT-1 cells were adoptively transferred into WT or *Batf3*$^{-/-}$ mice. Twenty-four hours later, 5×10^6 necrotic fibroblasts were injected (s.c.). Ninety hours later, draining lymph nodes were harvested, and OT-1 cell proliferation was determined by flow cytometry. The percentage of OT-1 cells (identified as $CD8^+CD45.1^+$) that divided at least once ($CFSE^{lo}$) is shown. The results are representative of three independent experiments. Each data point represents an individual animal. (Bars indicate mean values for each experimental group.)

Cross-Dressing Is a Robust Antigen Presentation Pathway in Vivo. To define the relative contribution of cross-presentation vs. cross-dressing in the response to vaccination, we generated C57BL/6→TAP$^{-/-}$ bone marrow (BM) chimeras. In these chimeras, vaccination with the K14-OVA DNA vaccine cannot generate OVA/K^b complexes from TAP$^{-/-}$ keratinocytes, eliminating cross-dressing but allowing cross-presentation of OVA protein by donor DCs as a route to T-cell activation. After adoptive transfer of CFSE-labeled OT-1 cells, BM chimeras were vaccinated with either a K14-OVA DNA vaccine or a K14-p5Y/ K^b SCT DNA vaccine (Fig. 4*A* and Fig. S7). Both DNA vaccines induced robust proliferation of OT-1 cells in BM chimeras (Fig. 4 *B* and *C*), suggesting that CD8$^+$ T-cell priming occurs by both cross-dressing and by cross-presentation in this model system.

Discussion

The studies reported here provide important insights into the importance of cross-dressing as a pathway for activation of CTLs. Using engineered SCT vaccines and *Batf3*-deficient mice, we demonstrate that cross-dressing is a robust pathway of cross-presentation, with the ability to prime both naïve and memory CTLs. Not only do these studies have important implications for the rational design of DNA and cellular vaccines, but they also have broader implications for understanding other immune responses generally considered to be dependent on cross-priming, such as viral infection and malignancy.

Our findings differ with Wakim and Bevan (4) in two ways. First, our data suggest that cross-dressed DCs can activate both naïve T cells and memory CD8$^+$ T cells. Following VSV infection, memory, but not naïve, CD8$^+$ T cells were activated by cross-dressed DCs (4). Conceivably, cross-dressing is inefficient following VSV infection relative to DNA or cell-based vaccination, resulting in low levels of antigen expression. Second, our data indicate that CD8α$^+$/CD103$^+$ DCs are required to prime CD8$^+$ T-cell responses by cross-dressing. Following lymphocytic choriomeningitis virus (LCMV) infection, cross-dressed CD8α$^-$ DCs are more efficient at stimulating a T-cell hybridoma ex vivo than cross-dressed CD8α$^+$ DCs (4), but in vitro studies have suggested that both CD8α$^-$ DCs and CD8α$^+$ DCs can acquire peptide–MHC complexes by cross-dressing (18). Anatomic location, cytokine production, or costimulatory receptors may also contribute to the in vivo capacity for CD8α$^+$ DCs to prime CD8$^+$ T-cell responses. It is possible that differences in experimental settings (viral infection vs. DNA vaccination vs. fibroblast injection) may explain the apparent conflict between our results and the results of Wakim and Bevan.

In addition, we have separately compared cross-presentation and cross-dressing in priming CD8$^+$ T-cell responses. After reconstitution of TAP$^{-/-}$ mice with C57BL/6 BM, we compared two DNA vaccination strategies using the same keratinocyte-specific promoter and model antigen. Both cross-presentation and cross-dressing pathways were able to induce similarly robust priming of CD8$^+$ T-cell responses, suggesting that cross-dressing

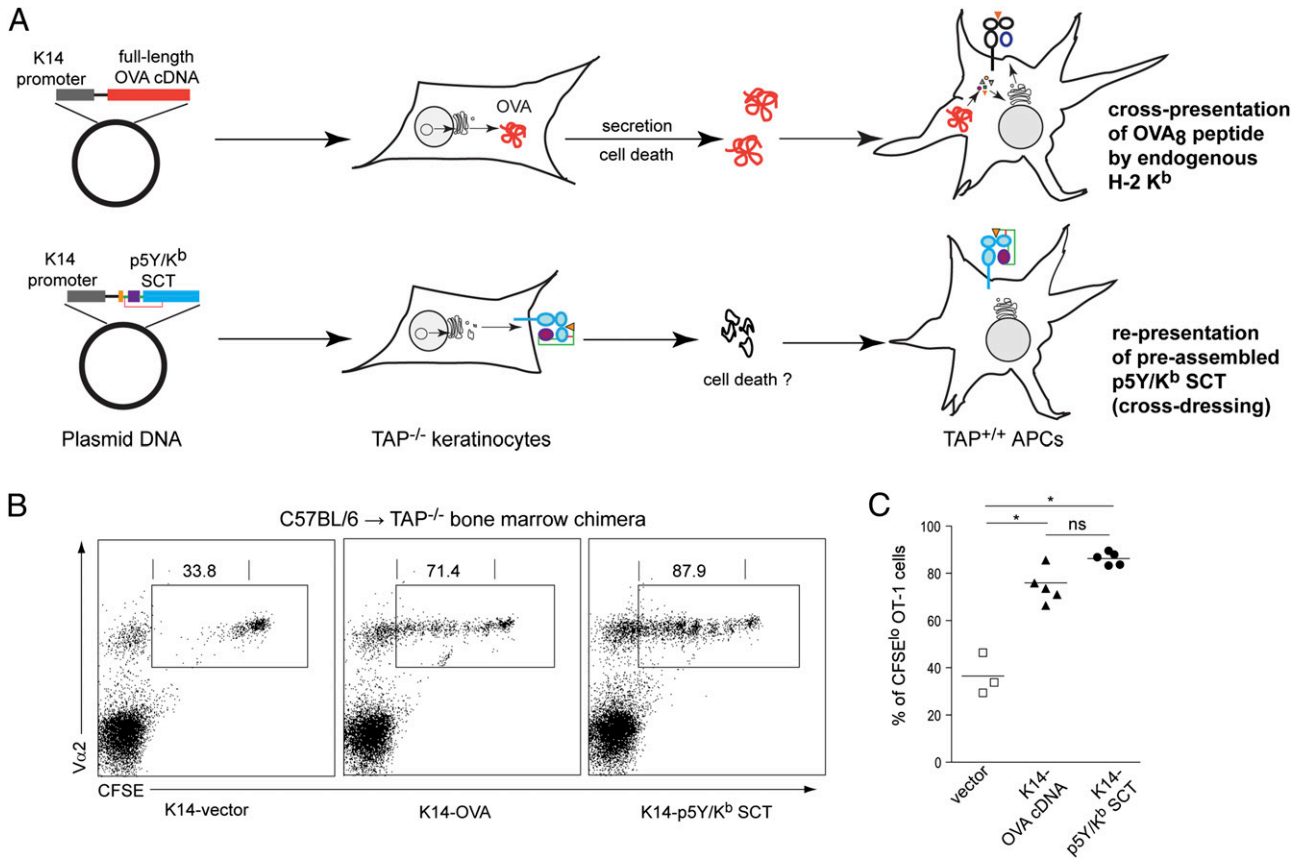

Fig. 4. Cross-dressing is a robust antigen-presentation pathway in vivo. CFSE-labeled OT-1 cells were adoptively transferred into the C57BL/6→TAP$^{-/-}$ BM chimeras, which were subsequently vaccinated with K14-OVA or K14-p5Y/K^b SCT. (*A*) This experimental model system results in CD8$^+$ T-cell priming by two distinct, nonoverlapping antigen-presentation pathways. (*B*) Spleen cells from vaccinated mice were collected and analyzed by flow cytometry. Representative two-color dot plots show expression of CFSE and Vα2 by viable CD8$^+$ T cells. Gated regions represent OT-1 cells (expressing CFSE, CD8, and Vα2). Numbers indicate the percentage of CFSE^{lo} OT-1 cells that had gone through at least one cell division. (*C*) Summary of data from individual animals (n = 3–5 per group). *$P < 0.01$; ns, not significant.

can be an important route of antigen presentation following vaccination. These studies also provide some insight into where cross-dressing may be occurring. Following vaccination with the K14 promoter construct, p5Y/K^b SCT expression is restricted to the dermis. Thus, exchange of intact p5Y/K^b SCT must occur in the periphery. Our data do not exclude the possibility that there is a second cross-dressing event that occurs in the lymph node.

Cross-priming is an important mechanism for activation of $CD8^+$ T cells that was first described over 25 y ago (19), and it is currently thought to proceed via cross-presentation rather than cross-dressing (4). Our results indicate otherwise, suggesting that cross-dressing can play an equally important role in $CD8^+$ T-cell priming. In addition, our studies have direct clinical implications, as strategies to optimize DNA and/or cellular vaccination depend critically on the pathway(s) of antigen presentation and the specific DC subtypes involved.

Materials and Methods

Animals. WT C57BL/6, 129SvEv, and $TAP^{-/-}$ mice were purchased from The Jackson Laboratory and Taconic, respectively. The generation of *Batf3*$^{-/-}$ mice on the 129SvEv background was described previously (5). For experiments involving OT-1 adoptive transfer, *Batf3*$^{-/-}$ backcrossed to C57BL/6 background for at least 10 generations were also used. HHD II mice (13, 15) are H-$2D^{b-/-}$ and $\beta_2m^{-/-}$ double knockout but express HLA-A2/H-$2D^b$ chimeric heavy chain covalently linked to human β_2m. OT-1 transgenic mice were originally purchased from The Jackson Laboratory and maintained as CD45.1 congenic by breeding to B6.SJL-*Ptprc*^{a}*Pepc*^{b}/BoyJ mice (The Jackson Laboratory). For some experiments, RAG2/OT-1 mice (Taconic) were used. All mice were bred and maintained in specific pathogen-free animal facilities according to institutional guidelines. Protocols were approved by the Animal Studies Committee at the Washington University School of Medicine. Generally, 8- to 12-wk-old sex and age-matched mice were used in the experiments.

DNA and Peptide Immunization. Full-length OVA cDNA was cloned into the pcDNA3.1(+) vector (Invitrogen) using standard techniques and was confirmed by DNA sequencing. Construction and progressive engineering of SCT has been described previously (6, 7, 9, 20). Mutations were introduced to SCT by site-directed mutagenesis (QuikChange II kit; Stratagene). DNA was administered by Helios gene gun (Bio-Rad) at 3-d intervals for a total of three doses. A total of 4 μg of DNA was delivered to nonoverlapping depilated abdominal skin with discharge helium pressure set to 400 psi. Primary immune responses were examined 5 d after the final vaccination. For DNA vaccination via intramuscular electroporation (EP), the TriGrid Delivery System (Ichor Medical Systems) was used. A total of 10 μg of DNA (20 μL) was injected (i.m.), followed by the application of a preprogrammed electric current. For peptide vaccination, 40 μg of OVA_8 peptide (AnaSpec) was mixed with the adjuvant TiterMax Gold (Sigma-Aldrich) and injected (s.c.) at the dorsal tail base.

Antibodies and Flow Cytometry. Fluorophore-labeled monoclonal antibodies were purchased from BD Bioscience, eBioscience, BioLegend, Miltenyi Biotec, and Dendritics. Antibody staining was generally performed in the presence of Fc block (BD). All flow cytometric data were collected on FACSCalibur or FACS Canto II instruments (BD Bioscience) and analyzed using FlowJo software (TreeStar).

ELISPOT Assay. IFN-γ ELISPOT assay was performed with reagents purchased from Mabtech unless otherwise noted. Briefly, 96-well PVDF filtration plates (Millipore) were coated overnight with 15 μg/mL capture antibody. Erythrocyte-free single-cell suspensions from the spleen were added in triplicate and incubated for 20 h with or without the presence of 1 μM OVA_8 peptide (AnaSpec). After extensive washes, 1 μg/mL biotinylated detection antibody was added. Streptavidin-alkaline phosphatase (ALP) and 5-bromo-4-chloro-3-indolyl phosphate/nitro blue tetrazolium (BCIP/NBT) (Moss Substrates) were subsequently used for color development. Plates were scanned and analyzed on an ImmunoSpot reader (C.T.L.).

Anti-OVA ELISA. Microtiter plates (96-well) (Corning) were coated with 150 μg/mL OVA (Sigma-Aldrich) and blocked. A total of 100 μL of immune sera (diluted 1:200) was added and incubated for 2 h. The plates were washed and HRP-conjugated goat anti-mouse IgG, IgG_1, or IgG_{2a} (Southern Biotech, diluted 1:5,000) were added and incubated for 1.5 h. The amount of bound OVA-specific Ab was determined by measuring the absorbance at 450 nm with a microplate reader (Bio-Rad; Model 550) after colorimetric development using 3,3′,5,5′- tetramethylbenzidine (TMB) substrate solution (Moss Substrates).

OT-1 T-Cell Isolation, CFSE Labeling, and Adoptive Transfer. Naïve OT-1 T cells were isolated from the spleens of transgenic mice using a $CD8^+$ T-cell enrichment kit (BD). Cells were labeled with 5 μM CFSE (Molecular Probes) at a concentration of 10×10^6/mL for 8 min. After quenching and extensive washing, cells were adoptively transferred to recipient mice via retroorbital injection.

Cell Culture. The 3KO MEFs were derived from a 16-d 3KO embryo (21) and maintained in DMEM with high glucose and L-glutamine (Invitrogen) supplemented with 10% (vol/vol) FBS (Atlanta Biologicals), Hepes, sodium pyruvate, nonessential amino acids, and antibiotic/antimycotic (all from Mediatech). Retroviruses encoding p5Y/K^b SCT were prepared (21) and used to transduce 3KO MEFs. Cells expressing high levels of SCT were selected and maintained in complete DMEM. DC2.4 (H-2^b genotype) cells were cultured in complete DMEM.

C57BL/6→$TAP^{-/-}$ Bone Marrow Chimera. BM cells were harvested from C57BL/6 mice. 15×10^6 cells were then injected i.v. into lethally irradiated (1,000 rad) recipient $TAP^{-/-}$ mice. Seven weeks later, CFSE-labeled OT-1 cells were adoptively transferred into the B6→$TAP^{-/-}$ BM chimeras, followed by DNA vaccination 24 h afterward.

Data Analysis. Data were analyzed using Prism 5 (GraphPad Software). An unpaired, two-tailed Student's *t* test was used to compare differences between groups, with $P \leq 0.05$ considered significant. Figures were exported and prepared using Adobe Illustrator CS3 (Adobe Systems).

ACKNOWLEDGMENTS. We thank Drs. Michael Bevan (University of Washington) and Paul Allen (Washington University) for critical review of the manuscript. We also thank Ichor Medical Systems for providing the TriGrid Delivery System and Dr. Thomas Griffith (University of Minnesota) for providing the Ad5.CMV-Flt3L viruses. This work was supported by Susan G. Komen for the Cure Grant KG080476 (to W.E.G. and L.L.), Department of Defense Grant W81XWH-06-1-0677 (to W.E.G.), National Institutes of Health Grant AI055849 (to T.H.H.); and grants from The Howard Hughes Medical Institute (to K.M.M.) and Frank Cancer Research Fund awarded by The Barnes–Jewish Hospital Foundation (to P.G.).

1. Kurts C, Robinson BW, Knolle PA (2010) Cross-priming in health and disease. *Nat Rev Immunol* 10:403–414.
2. Dolan BP, Gibbs KD, Jr., Ostrand-Rosenberg S (2006) Dendritic cells cross-dressed with peptide MHC class I complexes prime CD8+ T cells. *J Immunol* 177:6018–6024.
3. Dolan BP, Gibbs KD, Jr., Ostrand-Rosenberg S (2006) Tumor-specific CD4+ T cells are activated by "cross-dressed" dendritic cells presenting peptide-MHC class II complexes acquired from cell-based cancer vaccines. *J Immunol* 176:1447–1455.
4. Wakim LM, Bevan MJ (2011) Cross-dressed dendritic cells drive memory CD8+ T-cell activation after viral infection. *Nature* 471:629–632.
5. Hildner K, et al. (2008) Batf3 deficiency reveals a critical role for CD8alpha+ dendritic cells in cytotoxic T cell immunity. *Science* 322:1097–1100.
6. Yu YY, Netuschil N, Lybarger L, Connolly JM, Hansen TH (2002) Cutting edge: Single-chain trimers of MHC class I molecules form stable structures that potently stimulate antigen-specific T cells and B cells. *J Immunol* 168:3145–3149.
7. Li L, et al. (2010) Engineering superior DNA vaccines: MHC class I single chain trimers bypass antigen processing and enhance the immune response to low affinity antigens. *Vaccine* 28:1911–1918.
8. Mitaksov V, et al. (2007) Structural engineering of pMHC reagents for T cell vaccines and diagnostics. *Chem Biol* 14:909–922.
9. Truscott SM, et al. (2007) Disulfide bond engineering to trap peptides in the MHC class I binding groove. *J Immunol* 178:6280–6289.
10. Kim S, et al. (2005) Licensing of natural killer cells by host major histocompatibility complex class I molecules. *Nature* 436:709–713.
11. Choudhuri K, Wiseman D, Brown MH, Gould K, van der Merwe PA (2005) T-cell receptor triggering is critically dependent on the dimensions of its peptide-MHC ligand. *Nature* 436:578–582.
12. Wang B, et al. (2009) A single peptide-MHC complex positively selects a diverse and specific CD8 T cell repertoire. *Science* 326:871–874.
13. Kim S, et al. (2010) Single-chain HLA-A2 MHC trimers that incorporate an immundominant peptide elicit protective T cell immunity against lethal West Nile virus infection. *J Immunol* 184:4423–4430.
14. Connolly JM, Hansen TH, Ingold AL, Potter TA (1990) Recognition by CD8 on cytotoxic T lymphocytes is ablated by several substitutions in the class I alpha 3 domain: CD8 and the T-cell receptor recognize the same class I molecule. *Proc Natl Acad Sci USA* 87: 2137–2141.
15. Pascolo S, et al. (1997) HLA-A2.1-restricted education and cytolytic activity of CD8(+) T lymphocytes from beta2 microglobulin (beta2m) HLA-A2.1 monochain transgenic H-2Db beta2m double knockout mice. *J Exp Med* 185:2043–2051.

16. Howarth M, Williams A, Tolstrup AB, Elliott T (2004) Tapasin enhances MHC class I peptide presentation according to peptide half-life. *Proc Natl Acad Sci USA* 101: 11737–11742.
17. Vassar R, Rosenberg M, Ross S, Tyner A, Fuchs E (1989) Tissue-specific and differentiation-specific expression of a human K14 keratin gene in transgenic mice. *Proc Natl Acad Sci USA* 86:1563–1567.
18. Smyth LA, et al. (2008) The relative efficiency of acquisition of MHC:peptide complexes and cross-presentation depends on dendritic cell type. *J Immunol* 181:3212–3220.
19. Bevan MJ (1976) Cross-priming for a secondary cytotoxic response to minor H antigens with H-2 congenic cells which do not cross-react in the cytotoxic assay. *J Exp Med* 143:1283–1288.
20. Hansen T, Yu YY, Fremont DH (2009) Preparation of stable single-chain trimers engineered with peptide, β2 microglobulin, and MHC heavy chain. *Curr Protoc Immunol* 2009;Chapter 17:Unit17.5.
21. Lybarger L, Wang X, Harris MR, Virgin, HW, 4th, Hansen TH (2003) Virus subversion of the MHC class I peptide-loading complex. *Immunity* 18:121–130.